IMA Journal of Applied Mathematics (2020) **85**, 280–308
doi:10.1093/imamat/hxaa006
Advance Access publication on 18 March 2020

Multiple solutions and their asymptotics for laminar flows through a porous channel with different permeabilities

Hongxia Guo
Department of Applied Mathematics, School of Mathematics and Physics, University of Science and Technology, Beijing 100083, China

Changfeng Gui
Department of Mathematics, University of Texas at San Antonio, San Antonio, TX 78249, USA School of Mathematics and Statistics, The Central South University, Changsha 410083, China

Ping Lin*
Division of Mathematics, University of Dundee, Dundee, DD1 4HN, UK
*Corresponding author: p.lin@dundee.ac.uk

and

Mingfeng Zhao
Center for Applied Mathematics, Tianjin University, Tianjin, 300072, China

[Received on 16 April 2019; revised on 31 January 2020; accepted on 7 February 2020]

The existence and multiplicity of similarity solutions for the steady, incompressible and fully developed laminar flows in a uniformly porous channel with two permeable walls are investigated. We shall focus on the so-called asymmetric case where the upper wall is with an amount of flow injection and the lower wall with a different amount of suction. The numerical results suggest that there exist three solutions designated as type *I*, type *II* and type *III* for the asymmetric case, type *I* solution exists for all non-negative Reynolds number and types *II* and *III* solutions appear simultaneously at a common Reynolds number that depends on the value of asymmetric parameter a and with the increase of a the common Reynolds numbers are decreasing. We also theoretically show that there exist three solutions. The corresponding asymptotic solution for each of the multiple solutions is constructed by the method of boundary layer correction or matched asymptotic expansion for the most difficult high Reynolds number case. These asymptotic solutions are all verified by their corresponding numerical solutions.

Keywords: multiple solutions, laminar flows, boundary layers, singular perturbation method.

1. Introduction

Laminar flows in various geometries with porous walls are of fundamental importance to biological organisms, air circulation in the respiratory system, contaminant transports in aquifers and fractures, membrane filtration, control of boundary layer separation, transpiration cooling, propellant burning, automotive filters, etc. Hence, laminar flows through permeable walls have been extensively studied by researchers during the past several decades.

The analysis for Navier–Stokes equations that describe the two-dimensional steady laminar flows of a viscous incompressible fluid through a porous channel with uniform injection or suction was initiated by Berman (1953). He assumed that the flow is symmetric about the centre line of the channel and is of similarity form and reduced the problem to a fourth-order highly nonlinear ordinary differential equation with four boundary conditions and a cross-flow Reynolds number Re ($Re = \frac{dv_w}{\nu}$ depends on the

speed with which fluid is withdrawn from the channel, the half-width of the channel and the kinematic viscosity of the fluid). He also gave an asymptotic solution for small Reynolds number. Then, numerous studies have been done about the laminar flows in a channel or tube with permeable walls. Yuan (1956), Terrill & Shrestha (1965a) and Sellars (1955) obtained an asymptotic solution for the large injection and large suction cases, respectively. Terrill & Shrestha (1964, 1965a) and Shrestha (1967) derived a series of asymptotic solutions using the method of matched asymptotic expansion for the large injection and large suction cases with a transverse magnetic field.

All these works mentioned above had produced only one solution for each value of Re. Raithby (1971) was the first to find that there is a second solution for values of $Re > 12$ in a numerical investigation of the flow in a channel with heat transfer. Then, some studies were also devoted to the analysis of multiple solutions for the symmetric porous channel flow problem. Robinson (1976) conjectured that there are three types of solutions that were classified as type *I*, type *II* and type *III*. His conclusion was based on the numerical solutions and he also derived the asymptotic solutions of types *I* and *II* for the large suction case. Zaturska *et al.* (1988), Cox & King (1997) and Lu *et al.* (1992) also analyzed multiple solutions for the same problem. Robinson (1976) and Zaturska *et al.* (1988) pointed out that type *I* solution exists for all positive and negative Reynolds numbers, and types *II* and *III* solutions exist for $Re > Re^*$, where Zaturska *et al.* (1988) found $Re^* \approx 12.165$. Type *I* solution is increasing and concave down, type *II* solution is increasing with an inflection point, and type *III* solution is non-monotone with a turning point. Robinson (1976) pointed out that types *I* and *II* differ by exponentially small terms for the large suction Reynolds number and the inviscid solutions for them are all linear. Type *III* solution has a complicated structure, consisting of a viscous layer near the center line of the channel, a sinusoidal inviscid outer solution, a transition layer and a boundary layer (near the channel wall) for large suction Reynolds number. Lu (1997, 1999a,b) and MacGillivray & Lu (1994) mainly investigated the asymptotic solution of type *III*. It should be noted that only three solution branches are found for the porous channel flow due to the artificially imposed symmetry of the flow about the center line of the channel (i.e. considering the boundary conditions from the center line and the upper wall of channel). Hence, the solution is symmetric about the center line of channel which is the so-called symmetrical solution. Thus, possible asymmetric branches that could suddenly emerge would not be captured in the above approaches. Zaturska *et al.* (1988) showed that asymmetrical solutions can also be found when the full boundary value problem is solved (i.e. considering the boundary conditions from the upper and lower walls of channel). The asymmetrical solutions (Zaturska *et al.*, 1988, Cox & King, 2004) are available numerically for a more restricted range of Reynolds numbers than the symmetrical ones. Brady & Acrivos (1981) presented three symmetrical solutions for the flow in a channel or tube with an accelerating surface velocity.

In the same vein, the proof of solution multiplicity of Robinson's over different range of Reynolds number has been addressed by Shih (1987) who proved theoretically, applying a fixed point theorem, that there exists only one solution for injection case. Topological and shooting methods were used by Hastings *et al.* (1992) to prove the existence of all three of Robinson's conjectured solutions. He also presented the asymptotic behaviour for the flow as Re is large negative. Terrill (1965) proposed a transformation to convert the two-point boundary value problem into an initial value problem to facilitate the numerical calculation of solutions for an arbitrary Reynolds number. Based on the transformation proposed by Terrill (1965), Skalak & Wang (1978) described analytically the number and character of the solutions for each given Reynolds number under fairly general assumptions for the symmetrical channel and tube flow. The similar method was used by Cox (1991a) to analyze the symmetric solutions when the two walls are accelerating equally and when one wall is accelerating and the other is stationary. The uniqueness of similarity solution was investigated theoretically by Chellam & Liu (2006) and their work mainly considered the symmetric flow in a channel with slip boundary conditions. The temporal

stability issues of the solutions of Berman class continue to receive favour in the works of Zaturska *et al.* (1988), Cox (1991b), King & Cox (2001) and Watson *et al.* (1990, 1991). The spatial stability of steady solutions is another topic that has received much attention in the past. In that respect, one may count Varapaev & Yagodkin (1969), Brady (1984) and Durlofsky & Brady (1998). The asymptotic solutions of the laminar flow in a porous channel or tube with moving walls also received favour in the works of Majdalani & Zhou (2003), Dinarvand & Rashidi (2010) and Xu *et al.* (2010).

With unequal rates of suction or injection at the two walls, the steady solutions of the Berman problem are less well documented. The class of asymmetrical flows that may be driven by imposing different velocities on the walls turns out to be very interesting. The study of asymmetric laminar steady flow may be traced back to Proudman (1960) who found all possible inviscid outer solutions and identified the places where viscous layers necessarily form. Then, Terrill & Shrestha (1966, 1965b) and Shrestha & Terrill (1968) extended Proudman's work and constructed one asymptotic solution using the method of matched asymptotic expansion for the large injection, large suction and mixed cases, respectively. Here the mixed cases mean that one wall is with injection while the other is with suction. Cox (1991b) considered the practical case of an impermeable wall opposing a transpiring wall. Watson *et al.* (1991) also investigated the case of asymmetrical flow in a channel where one wall is stationary and the other is accelerating. Cox & King (2004) constructed asymmetrical asymptotic solution of the symmetric problem for the large suction Reynolds number case and asymptotic multiple solutions of the asymmetric problem in which fluid flows through a channel with different suction velocities on each wall. King & Cox (2005) constructed the asymptotic solutions with stagnation point for the fluid flows near a permeable wall for large suction or injection case.

The purpose of this paper is not to reconsider any of these previously considered problems, but instead to provide a thorough analysis for the asymmetric flow in a channel of porous walls with different permeabilities, where the upper wall is with injection and the lower wall is with suction. We will show that there exist three multiple solutions in this asymmetric case. We also mark them as type *I*, type *II* and type *III* solutions as people do for the symmetric case. We should remark here that type *I*, type *II* and type *III* solutions for the asymmetric case are much different from those for the symmetric case. We will numerically give the range of the Reynolds number where there exist three solutions. We will then construct asymptotic solutions for each solution for the most difficult case of high Reynolds number and numerically validate the constructed solutions. The paper is organized as follows. In Section 2, by applying mass conservation (Dauenhauer, 2003; Bouyges *et al.*, 2017), a similar equation can be developed. Hence, a similarity transformation is introduced and the Navier–Stokes equations are reduced to a single fourth-order nonlinear ordinary differential equation with a Reynolds number *Re* and four boundary conditions. In Section 3, we compute the multiple solutions numerically. We also sketch velocity profiles and streamlines for these asymmetric flows. In Section 4, we theoretically analyze that there exist three solutions of similarity transformed equation under fairly general assumptions. In Section 5, for the most difficult high Reynolds number case, the asymptotic solution for each type of multiple solutions will be constructed using the method of boundary layer correction or matched asymptotic expansion. In Section 6, all the asymptotic solutions are verified by numerical solutions and meanwhile these asymptotic solutions may serve as a validation for the numerical method used in the paper.

2. Mathematical formulation

As shown in Fig. 1, we consider the 2D, steady, incompressible asymmetric laminar flows in a porous and elongated rectangular channel. The channel exhibits a sufficiently small depth-width ratio of semi-

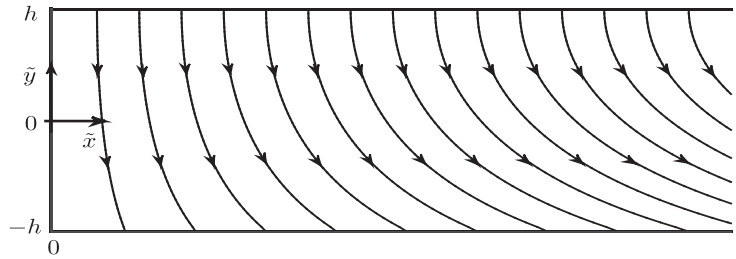

FIG. 1. Coordinate system and characteristic streamlines used to describe the fluid flow pattern.

height h to length L. Despite the channel's finite body length, it is reasonable to assume a semi-infinite length in order to neglect the influence of the opening at the end (Uchida & Aoki, 1977). The flow is driven by uniform injection through the upper wall of the channel with speed $-v_2$ and uniform suction through the lower wall with speed $-v_1$, where we assume $v_2 > 0$ and $v_1 > 0$. We define a parameter $a = \frac{v_1}{v_2}$, where $a > 0$, to describe the asymmetry. Let $\tilde{x}$ and $\tilde{y}$ be chosen as the coordinates measured along and perpendicular to the flow direction, respectively and u and v be the velocity components in the direction of $\tilde{x}$ and $\tilde{y}$ increasing, respectively. The streamwise velocity is zero at the closed headend ($\tilde{x} = 0$).

The equations of the continuity and momentum for the steady laminar flows of an incompressible Newtonian fluid through a porous channel are (Terrill & Shrestha, 1966)

$$\nabla \cdot \mathbf{V} = 0, \tag{2.1}$$

$$(\mathbf{V} \cdot \nabla)\mathbf{V} = -\frac{1}{\rho}\nabla p + \nu \nabla^2 \mathbf{V}, \tag{2.2}$$

where the symbol $\mathbf{V} = (u(\tilde{x}, \tilde{y}), v(\tilde{x}, \tilde{y}))$ represents the velocity vector, p the pressure, ρ the density and ν the kinematic viscosity of the fluid. The boundary conditions necessary for describing the asymmetric flow and solving the continuity and momentum equations are

$$u(0, \tilde{y}) = 0, \tag{2.3}$$

$$u(\tilde{x}, -h) = 0, \quad v(\tilde{x}, -h) = -v_1, \tag{2.4}$$

$$u(\tilde{x}, h) = 0, \qquad v(\tilde{x}, h) = -v_2. \tag{2.5}$$

By applying the mass conservation to a volume of fluid extending from the headend ($\tilde{x} = 0$) to an arbitrary location $\tilde{x}$, the flow velocity $u_m(\tilde{x})$ spatially averaged over the cross section can be found to be proportion to $\tilde{x}$ (Dauenhauer, 2003; Bouyges *et al.*, 2017). To that end, the mean flow velocity u_m must be determined from

$$A_{cs} \cdot u_m(\tilde{x}) = \int_{A_{cs}} \mathbf{u}(\tilde{x}, \tilde{y}) \cdot \mathrm{d}\mathbf{A}, \tag{2.6}$$

where $A_{cs} = 2hz$ is the surface area of the cross section and z is the length of $\tilde{z}$ coordinate. However, since $A_{uw} = \tilde{x}z$ is the porous area of channel's upper wall, $A_{lw} = \tilde{x}z$ is the porous area of channel's lower wall, and the headend wall is not porous by the boundary condition (2.3), mass conservation requires that

$$\rho A_{uw} v_2 - \rho A_{lw} v_1 - \int_{A_{cs}} \rho \mathbf{u}(\tilde{x}, \tilde{y}) \cdot \mathrm{d}\mathbf{A} = 0. \tag{2.7}$$

Combining (2.6) and (2.7), one can obtain

$$u_m = \frac{A_{uw}}{A_{cs}} v_2 - \frac{A_{lw}}{A_{cs}} v_1 = \frac{\tilde{x}}{2h}(v_2 - v_1). \tag{2.8}$$

A sufficient condition for u to satisfy the mass conservation (2.7) is to assume a linear variation with respect to $\tilde{x}$. To make further headway, only separable product solutions are sought, thus turning the linear dependence on $\tilde{x}$ into a necessary condition. Therefore, a self-similarity transformation that can result in such a variation is desirable. On the other hand, as we know, the study of the fluid flow equations with a high Reynolds number (which will be mentioned next in (2.16)) is most challenging. A similarity transformation provides a way to explicitly express the solutions for the channel flow. Furthermore, for the physical applications, such explicit solutions are often preferred in understanding the fluid properties especially the boundary layers. For these purposes, we introduce a streamfunction and express the velocity components in terms of the streamfunction

$$u = \frac{\partial \psi}{\partial \tilde{y}}, \quad v = -\frac{\partial \psi}{\partial \tilde{x}}. \tag{2.9}$$

From this definition of the streamfunction, the continuity (2.1) is naturally satisfied. Then, taking the curl of the momentum equation deduces the vorticity transport equation

$$u\frac{\partial \omega}{\partial \tilde{x}} + v\frac{\partial \omega}{\partial \tilde{y}} = \nu\left(\frac{\partial^2 \omega}{\partial \tilde{x}^2} + \frac{\partial^2 \omega}{\partial \tilde{y}^2}\right), \tag{2.10}$$

where

$$\omega = \frac{\partial v}{\partial \tilde{x}} - \frac{\partial u}{\partial \tilde{y}} = -\nabla^2 \psi. \tag{2.11}$$

Substituting (2.9) and (2.11) into (2.10), one can obtain

$$\frac{\partial \psi}{\partial \tilde{y}}\frac{\partial}{\partial \tilde{x}}\nabla^2 \psi - \frac{\partial \psi}{\partial \tilde{x}}\frac{\partial}{\partial \tilde{y}}\nabla^2 \psi = \nu \nabla^2 \nabla^2 \psi. \tag{2.12}$$

Then, we introduce a streamfunction of the form

$$\psi = \nu x F(y), \tag{2.13}$$

where $x = \frac{\tilde{x}}{h}$, $y = \frac{\tilde{y}}{h}$ which are the non-dimensional coordinates and $F(y)$ is independent to the streamwise coordinate. Then, the velocity components are given by

$$u = \frac{\nu x}{h} F'(y), \quad v = -\frac{\nu}{h} F(y). \tag{2.14}$$

Substituting (2.13) into (2.12), a fourth-order nonlinear ordinary differential equation with a parameter Re is developed. It is

$$f^{iv} + Re(ff''' - f'f'') = 0, \tag{2.15}$$

where $Re = \frac{hv_2}{\nu}$ is the Reynolds number based on the fluid velocity v_2 through the upper wall and the semi-height h of channel and $f(y) = \frac{F(y)}{Re}$. A first integral of (2.15) is

$$f''' + Re(ff'' - f'^2) = K, \tag{2.16}$$

where K is an undetermined integration constant.

The boundary conditions of no-slip given by (2.4) and (2.5) can now be updated to the normalized form

$$f(-1) = a,\ f'(-1) = 0,\ f(1) = 1,\ f'(1) = 0. \tag{2.17}$$

We shall seek all possible solutions to the boundary value problem (2.15) or (2.16) and (2.17) for all non-negative values of Reynolds numbers that correspond to the flow permeating from upper wall of the porous channel and exiting from the lower wall with different permeabilities. The negative Reynolds numbers are permissible, correspond to the flow through the walls of channel possibly with a different suction velocity at each wall and have been investigated by Cox & King (2004).

3. Numerical multiple solutions

Numerical solutions to (2.15) or (2.16) subject to (2.17) are considered for all non-negative Reynolds number, $0 \leqslant Re < \infty$. All the numerical results are based on the collocation method (e.g. MATLAB boundary value problem solver bvp4c in which we set the relative error tolerance 10^{-6}). The numerical results are shown in Fig. 2 with a plot of skin friction at the lower wall $-f''(-1)$ versus Reynolds number Re at $a = 0.4$, $a = 0.6$ and $a = 0.8$, respectively. The solution curves have been labeled *I*, *II* and *III* suggesting three completely different types of solutions. The type *I* extends over $0 \leqslant Re < \infty$, in what follows, the common points Re of types *II* and *III* will be taken to be $Re = 38.819$ at $a = 0.4$, $Re = 21.145$ at $a = 0.6$ and $Re = 14.074$ at $a = 0.8$. For the symmetric flow in a channel, although there are three types of solutions, two of them have only an exponentially small difference when Re is large (Robinson, 1976; Brady & Acrivos, 1981). In the following, we will present the velocity components and streamlines of the three types solutions with several Reynolds numbers at $a = 0.8$.

Typical velocity profiles of type *I* solution, i.e. $v \sim f(y)$ and $u \sim xf'(y)$, are shown in Fig. 3. As can be seen from the streamwise velocity, the flows form a thin boundary layer structure near the lower wall of the channel for the relatively high Reynolds number. The increasing Reynolds number has little influence on the flow character, but the boundary layer is thinner and thinner with the increase of Re.

Typical velocity profiles for type *II* solution are presented in Fig. 4. All of these flows occur as $Re > 14.074$ at $a = 0.8$. As Re is increased, the minimum of transverse velocity in the reverse region is decreasing and the turning points which are the points such that $f(y) = 0$ are moving towards the walls

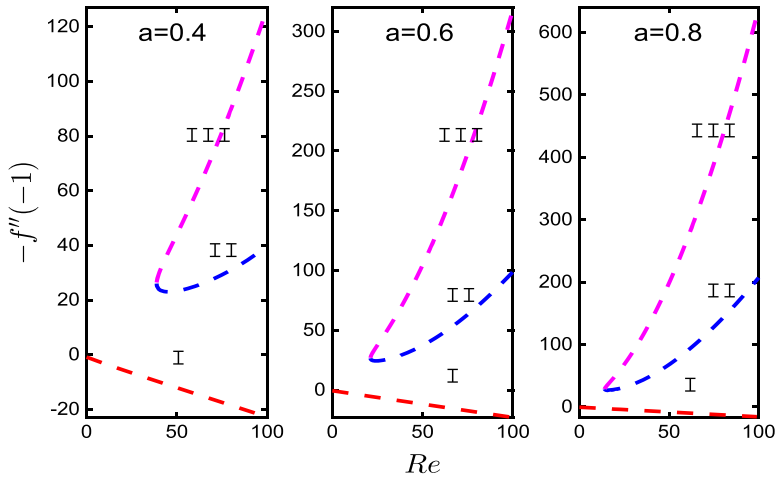

FIG. 2. Skin friction at the lower wall versus crossflow Reynolds number for the flow through a uniformly porous channel at $a = 0.4$, $a = 0.6$ and $a = 0.8$, respectively.

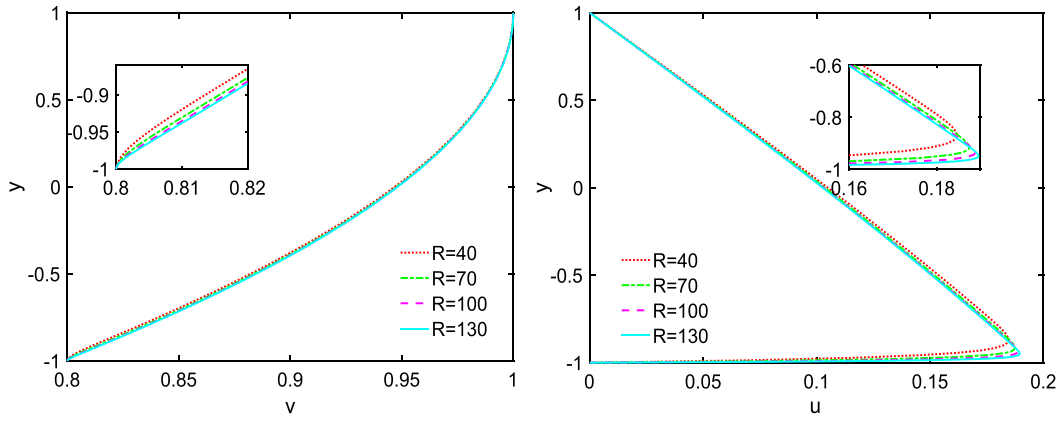

(a) Transverse velocity of type *I* (b) Streamwise velocity of type *I*

FIG. 3. Velocity profiles of type *I* at $a = 0.8$ with $Re = 40$, $Re = 70$, $Re = 100$ and $Re = 130$.

of the channel. The maximum of streamwise velocity is increasing and the minimum is decreasing with the increase of *Re*.

The type *III* solutions, shown in Fig. 5, have an unusual shape. The rapid decay occurs not only for the streamwise velocity but also for the transverse velocity near the lower wall. With the increase of *Re*, the region between the lower wall and the minimum velocity becomes thinner. There is a region of reverse flow near the lower wall for the streamwise velocity.

All numerical results indicate that the solutions contain inviscid solution and boundary layer solution that is confined to the viscous layer near the lower wall of the channel. It is obvious that the flow direction of streamwise velocity inside the boundary layers for types *II* and *III* is opposite to the type *I*. The reversal flow occurs for both types *II* and *III*.

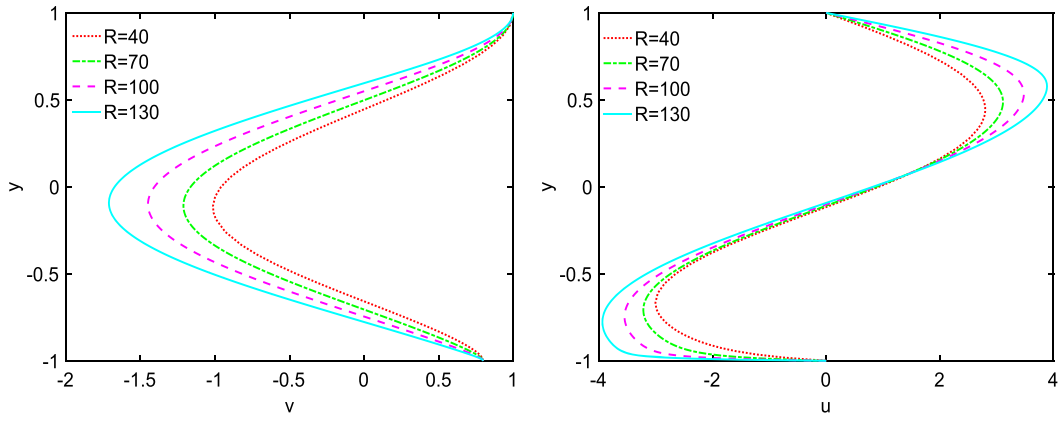

(a) Transverse velocity of type *II* (b) Streamwise velocity of type *II*

FIG. 4. Velocity profiles of type *II* at $a = 0.8$ with $Re = 40$, $Re = 70$, $Re = 100$ and $Re = 130$.

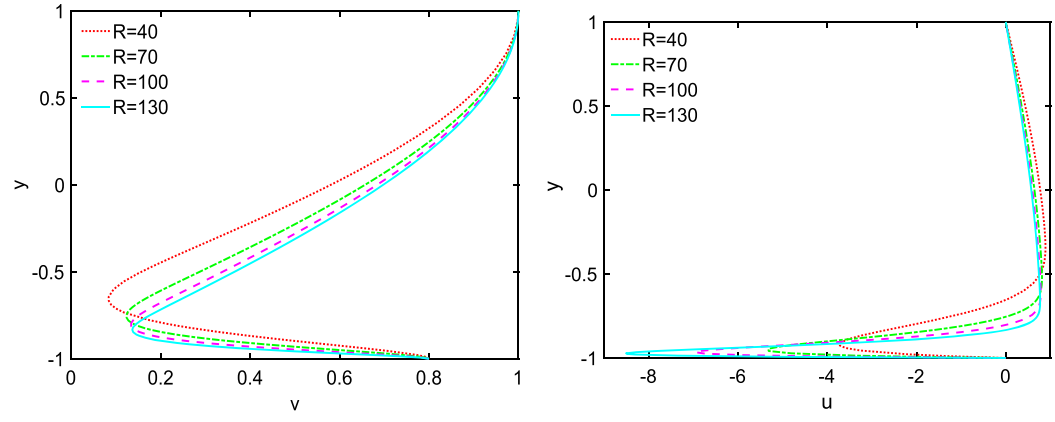

(a) Transverse velocity of type *III* (b) Streamwise velocity of type *III*

FIG. 5. Velocity profiles of type *III* at $a = 0.8$ with $Re = 40$, $Re = 70$, $Re = 100$ and $Re = 130$.

In an effort to develop a better understanding of the flow character, we show in Fig. 6 sketches of the streamlines to describe the flow behaviour corresponding to different branches of solutions. These graphs depict all three types of solutions and enable us to deduce their fundamental characteristics. The type *I* streamlines, we can clearly see that the injection at the upper wall push the streamlines closer to the lower wall and the suction at the lower wall draws them somewhat away from the lower wall. The type *II* streamlines indicate that the fluid that is injected at the upper wall goes off to infinity; the central region involves fluid coming in from infinity then returning to infinity; the lower wall withdraws fluid that comes from infinity (in particular, the fluid that is injected at the upper wall is not the same fluid as withdrawn at the lower wall). The type *III* streamlines indicate that the fluid that is injected at the upper wall goes closely to the lower wall and then goes off to infinity; the lower wall withdraws fluid that comes from infinity (in particular, the fluid that is injected at the upper wall is the same

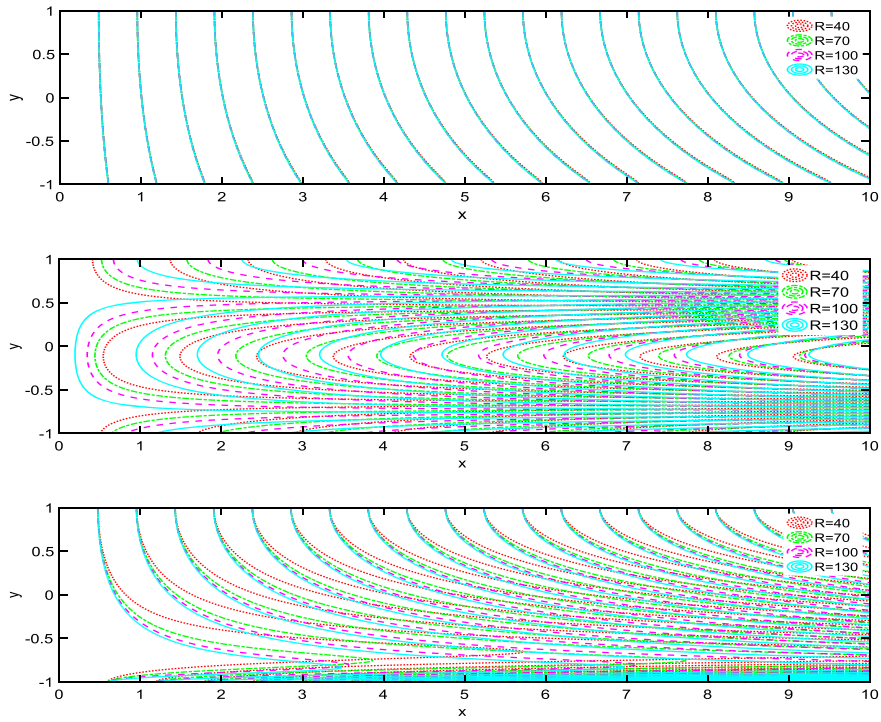

FIG. 6. Streamline patterns of types *I*, *II* and *III* solutions from top to bottom at $a = 0.8$ with $Re = 40$, $Re = 70$, $Re = 100$ and $Re = 130$.

fluid as withdrawn at the lower wall). For the types *II* and *III* streamlines, in the same vein, the large injection promotes a more abrupt change in the flow direction from streamwise to normal. This tends to be accompanied by sharper flow turning near the wall. These differences in streamline curvature, and hence, the flow turning rate, become more appreciable when we focus our attention further right hand of the channel.

4. Existence of multiple solutions

Skalak & Wang (1978), Cox (1991a) and Chellam & Liu (2006) considered symmetric flow in a channel with porous walls, accelerating walls and slip boundary conditions, respectively. In this section, we extend previous analysis (Skalak & Wang, 1978; Cox, 1991a, Chellam & Liu, 2006) to investigate asymmetric flow in a porous channel with different permeabilities and to discuss the existence of multiple solutions.

The two-point boundary value problem, (2.16) and (2.17), can be converted into an initial value problem. Rescalling (2.16) and (2.17) by introducing $f(y) = \frac{1}{2}bg(\xi)/Re$ and $\xi = \frac{1}{2}b(y+1)$ (Terrill, 1965; Skalak & Wang, 1978):

$$g''' + gg'' - g'^2 = \chi, \tag{4.1}$$

$$g(0) = \frac{2aRe}{b},\ g'(0) = 0,\ g(b) = \frac{2Re}{b},\ g'(b) = 0, \tag{4.2}$$

where $\chi = \frac{16RK}{b^4}$, $a > 0$, $b > 0$ and $Re > 0$. Assume all the initial conditions of (4.1) can be

$$g(0) = 2aRe/b, \quad g'(0) = 0, \quad g''(0) = A, \quad g'''(0) = B, \tag{4.3}$$

where $A, B \neq 0$. If we find a point ξ^* such that $g'(\xi) = 0$, we obtain b by setting $\xi^* = b$ and the value of $g(b)$ at this point gives the Reynolds number $Re = \frac{1}{2}bg(b)$. Then, we can obtain the original solution $f(y)$. Since for our physical model, our analysis is restricted to positive Re, there must be $g(b) > 0$ (i.e. $g(\xi^*) > 0$). Thus, we will discuss analytically the number of possible roots ξ^* of $g'(\xi)$ (each with $g(\xi^*) > 0$), which is based on the signs of A and B, covering the entire range of $\xi > 0$.

Let $h_1(\xi) = g'(\xi)$, $h_2(\xi) = g''(\xi)$, $h_3(\xi) = h'''(\xi)$, $h_4(\xi) = g^{(4)}(\xi)$ and $h_5(\xi) = g^{(5)}(\xi)$ for all $\xi \geqslant 0$. Differentiate (4.1) twice

$$h_4 = h_1h_2 - gh_3, \tag{4.4}$$

$$h_5 + gh_4 = (h_2)^2. \tag{4.5}$$

LEMMA 4.1 If $B < 0$, then $g^{(4)}(\xi) > 0$ for all $\xi \geqslant 0$. In particular, $g'''(\xi)$ is a strictly increasing function of ξ on $[0, +\infty)$.

Proof. By (4.4), since $g'(0) = 0$, then $h_4(0) = g'(0)g''(0) - g(0)h_3(0) = -g(0)B$. Since $g(0) > 0$ and $B < 0$, then $h_4(0) > 0$. By (4.5), then $h_4' + gh_4 \geqslant 0$ for all $\xi \geqslant 0$, i.e. $\left(e^{\int_0^\xi g(t)\mathrm{d}t}h_4(\xi)\right)' \geqslant 0$ for all $\xi \geqslant 0$, which implies that $e^{\int_0^\xi g(t)\mathrm{d}t}h_4(\xi) \geqslant h_4(0) > 0$ for all $\xi \geqslant 0$. Hence $h_4(\xi) = g^{(4)}(\xi) > 0$ for all $\xi \geqslant 0$. □

REMARK 4.1 The proof of Lemma 4.1 only uses the condition $g(0)B < 0$.

PROPOSITION 4.1 Assume that $A > 0$ and $B < 0$.

(a) If there exists some $x_0 > 0$ such that $g'''(x_0) = 0$, then there is no point $\zeta > x_0$ such that $g'(\zeta) = 0$ and $g(\zeta) > 0$.

(b) If $g'''(\xi) < 0$ for all $\xi \geqslant 0$ and $h_2(\alpha) = 0$ for some $\alpha > 0$, then there exists some $\zeta > \alpha$ such that $g'(\zeta) = 0$ and $g(\zeta) > 0$.

Proof. (a) By Lemma 4.1, then $h_4(\xi) > 0$ for all $\xi \geqslant 0$. Since $h_3(x_0) = 0$, then $h_3(\xi) < 0$ for all $\xi \in [0, x_0)$ and $h_3(\xi) > 0$ for all $\xi > x_0$, which implies that $h_2(\xi)$ is strictly decreasing on $[0, x_0)$ and strictly increasing on $(x_0, +\infty)$. Hence x_0 is the unique global minimum point of $h_2(\xi)$ on $[0, +\infty)$. Since $h_3(x_0) = 0$, by (4.4) and Lemma 4.1, then $h_4(x_0) = h_1(x_0)h_2(x_0) - g(x_0)h_3(x_0) = h_1(x_0)h_2(x_0) > 0$. Let us assume that there is some $\zeta > x_0$ such that $h_1(\zeta) = g'(\zeta) = 0$ and $g(\zeta) > 0$. Since $g'(0) = g'(\zeta) = 0$, by Lagrange's mean value theorem, then there exists some $\alpha \in (0, \zeta)$ such that $h_2(\alpha) = 0$. Since x_0 is the unique global minimum point of $h_2(\xi)$ on $[0, +\infty)$ and $h_2(x_0) \neq 0$, then $h_2(x_0) < 0$. Since $h_4(\xi) > 0$ for all $\xi \geqslant 0$ and $h_3(\xi) > 0$ for all $\xi > x_0$, then $\lim_{\xi \to +\infty} h_2(\xi) = +\infty$. Since $h_2(0) = A > 0$, $h_2(x_0) < 0$ and $h_4(\xi) > 0$ for all $\xi \geqslant 0$, then there exists a unique $\beta > x_0$ such that $h_2(\xi) < 0$ for all $\alpha < \xi < \beta$, and $h_2(\xi) > 0$ for all $0 \leqslant \xi < \alpha$ and all $\xi > \beta$. Since $h_1(x_0)h_2(x_0) > 0$ and $h_2(x_0) < 0$, then $h_1(x_0) < 0$. Since $h_1(\zeta) = 0$, by (4.4), then $h_4(\zeta) = h_1(\zeta)h_2(\zeta) - g(\zeta)h_3(\zeta) = -g(\zeta)h_3(\zeta)$. Since $h_4(\xi) > 0$ for all $\xi > 0$ and $g(\zeta) > 0$, then $h_3(\zeta) < 0$, which implies that $\zeta < x_0$, this leads to a contradiction.

(b) Since $g'''(\xi) < 0$ for all $\xi \geqslant 0$ and $h_2(\alpha) = 0$ for some $\alpha > 0$, then $h_2(\xi) > 0$ for all $0 \leqslant \xi < \alpha$ and $h_2(\xi) < 0$ for all $\xi > \alpha$, which implies that $h_1(\xi)$ is strictly increasing on $[0, \alpha)$ and strictly decreasing on $(\alpha, +\infty)$. Hence α is the unique global maximum point of $h_1(\xi)$ on $[0, +\infty)$. Since $h_1(0) = 0$, then $h_1(\alpha) > 0$. Since $h_2(\xi) < 0$ for all $\xi > \alpha$ and $h_3(\xi) < 0$ for all $\xi \geqslant 0$, then $\lim_{\xi \to +\infty} h_1(\xi) = -\infty$. Since $h_1(\alpha) > 0$ and $h_2(\xi) < 0$ for all $\xi > \alpha$, then there exists a unique $\zeta > \alpha$ such that $g'(\zeta) = h_1(\zeta) = 0$. Since $h_1(\zeta) = 0$, by e(4.4), then $h_4(\zeta) = h_1(\zeta)h_2(\zeta) - g(\zeta)h_3(\zeta) = -g(\zeta)h_3(\zeta)$. Since $\zeta > \alpha$, $h_3(\xi) < 0$ for all $\xi \geqslant 0$ and Lemma 4.1, then $g(\zeta) > 0$. Therefore, in this case, there exists a solution of (2.16) and (2.17). We will designate this solution as type *I* solution corresponding to the numerical type *I* solution in Section 3. □

PROPOSITION 4.2 Assume that $A < 0$ and $B < 0$.

(a) Then there exists some $x_0 > 0$ such that $g'''(x_0) = 0$.

(b) Then there is no point $\zeta > 0$ such that $g'(\zeta) = 0$ and $g(\zeta) > 0$.

Proof. (a) If the statement is not right, since $B = g'''(0) < 0$, then $h_3(\xi) < 0$ for all $\xi \geqslant 0$. Since $A = g''(0) < 0$, then $h_2(\xi) \leqslant A < 0$ for all $\xi \geqslant 0$, which implies that $h_1(\xi) - h_1(0) \leqslant A\xi$ for all $\xi \geqslant 0$. Since $h_1(0) = 0$, then $h_1(\xi) < 0$ and $h_1(\xi) \leqslant A\xi$ for all $\xi \geqslant 0$, which implies that $g(\xi) - g(0) \leqslant \frac{A}{2}\xi^2$ for all $\xi \geqslant 0$. Hence $\lim_{\xi \to +\infty} g(\xi) = -\infty$. By (4.5), then $h_5 = (h_2)^2 - gh_4$ for all $\xi \geqslant 0$. By Lemma 4.1, then $h_4(\xi) > 0$ for all $\xi \geqslant 0$. Since $\lim_{\xi \to +\infty} g(\xi) = -\infty$, then there exists some $M > 0$ such that $h_5(\xi) > 0$ for all $\xi \geqslant M$. Since $h_4(\xi) > 0$ and $h_5(\xi) > 0$ for all $\xi \geqslant M$, then $\lim_{\xi \to +\infty} h_3(\xi) = +\infty$, this leads to a contradiction.

(b) By the result of part (a) then there exists some $x_0 > 0$ such that $g'''(x_0) = 0$. Since $h_4(\xi) \geqslant 0$ for all $\xi \geqslant 0$, then $h_3(\xi) < 0$ for all $\xi \in [0, x_0)$ and $h_3(\xi) > 0$ for all $\xi > x_0$, which implies that $h_2(\xi)$ is strictly decreasing on $[0, x_0)$ and strictly increasing on $(x_0, +\infty)$. Hence x_0 is the unique global minimum point of $h_2(\xi)$ on $[0, +\infty)$. Since $g''(0) = A < 0$ and $h_3(\xi) < 0$ for all $\xi \in [0, x_0)$, then $h_2(\xi) < A < 0$ for all $\xi \in (0, x_0]$. Since $h_1(0) = 0$, then $h_1(\xi) \leqslant A\xi < 0$ for all $\xi \in (0, x_0]$. Since $h_3(\xi) > 0$ for all $\xi > x_0$ and $h_4(\xi) > 0$ for all $\xi \geqslant 0$, then $\lim_{\xi \to +\infty} h_2(\xi) = +\infty$. Since $h_2(x_0) < 0$ and $h_3(\xi) > 0$ for all $\xi > x_0$, then there exists a unique $x_1 > x_0$ such that $h_2(\xi) < 0$ for all $\xi \in [x_0, x_1)$, $h_2(x_1) = 0$ and $h_2(\xi) > 0$ for all $\xi > x_1$. Since $h_2(\xi) < A < 0$ for all $\xi \in (0, x_0]$, then $h_2(\xi) < 0$ for all $0 \leqslant \xi < x_1$ and $h_2(\xi) > 0$ for all $\xi > x_1$, which implies that $h_1(\xi)$ is strictly decreasing on $[0, x_1]$ and strictly increasing on $[x_1, +\infty)$. Hence x_1 is the unique global minimum point of $h_1(\xi)$ on $[0, +\infty)$. Since $h_1(\xi) \leqslant A\xi < 0$ for all $\xi \in (0, x_0]$, then $h_1(x_1) < 0$. Since $h_2(\xi) > 0$ for all $\xi > x_1$ and $h_3(\xi) > 0$ for all $\xi > x_0$, then $\lim_{\xi \to +\infty} h_1(\xi) = +\infty$. Since $h_1(\xi) < 0$ for all $0 < \xi \leqslant x_1$ and $h_2(\xi) > 0$ for all $\xi > x_1$, then there exists a unique $x_2 > x_1$ such that $h_1(x_2) = 0$. So we know that x_2 is the unique solution of $h_1(\xi) = 0$ for all $\xi > 0$. On the other hand, since $x_2 > x_1 > x_0$, then $h_4(x_2) > 0$ and $h_3(x_2) > 0$. Since $h_1(x_2) = 0$, by (4.4), then $h_4(x_2) = h_1(x_2)h_2(x_2) - g(x_2)h_3(x_2) = -g(x_2)h_3(x_2) > 0$. Since $h_3(x_2) > 0$, then $g(x_2) < 0$. Since x_2 is the unique solution of $h_1(\xi) = 0$ for all $\xi > 0$, and $g(x_2) < 0$, then there is no point $\zeta > 0$ such that $g'(\zeta) = 0$ and $g(\zeta) > 0$. □

PROPOSITION 4.3 Assume that $B > 0$.

(a) If $h_4(\xi) \neq 0$ for all $\xi > 0$, then $h_4(\xi) < 0$ for all $\xi \leqslant 0$.

(b) If $h_4(\xi_0) = 0$ for some $\xi_0 > 0$, then $h_4(\xi) < 0$ for all $0 \leqslant \xi < \xi_0$ and $h_4(\xi) > 0$ for all $\xi > \xi_0$.

Proof. (a) By (4.4), since $g'(0) = 0$, then $h_4(0) = h_1(0)h_2(0) - g(0)h_3(0) = -g(0)B$. Since $g(0) > 0$ and $B > 0$, then $h_4(0) < 0$. By the assumption that $h_4(\xi) \neq 0$ for all $\xi > 0$, then $h_4(\xi) < 0$ for all $\xi \leqslant 0$.

(b) By the proof of part (a), we know that $h_4(0) < 0$. Let $\Sigma = \{\xi > 0 : h_4(\xi) = 0\}$, by the assumption, then $\xi_0 \in \Sigma$. Since $h_4(0) < 0$, by the continuity, we know that $\eta := \inf_{\xi\in\Sigma} \xi \in (0, \xi_0]$, which implies that $\xi_0 \geqslant \eta$, $h_4(\eta) = 0$ and $h_4(\xi) < 0$ for all $0 \leqslant \xi < \eta$. By (4.5), then $h_4' + gh_4 \geqslant 0$ for all $\xi \geqslant 0$, i.e. $\left(e^{\int_\eta^\xi g(t)\mathrm{d}t} h_4(\xi)\right)' \geqslant 0$ for all $\xi \geqslant 0$, which implies that $e^{\int_\eta^\xi g(t)\mathrm{d}t} h_4(\xi) \geqslant h_4(\eta) = 0$ for all $\xi \geqslant \eta$. Hence $h_4(\xi) = g^{(4)}(\xi) \geqslant 0$ for all $\xi \geqslant \eta$.

Claim 4.4 $h_4(\xi) > 0$ for all $\xi > \eta$. □

Proof. If not, since $h_4(\xi) \geqslant 0$ for all $\xi \geqslant \eta$, then there exists some $\alpha > \eta$ such that $h_4(\alpha) = 0$. If $h_4(\xi) \equiv 0$ for all $\eta \leqslant \xi \leqslant \alpha$, by (4.5), then $h_2(\xi) \equiv 0$ for all $\eta \leqslant \xi \leqslant \alpha$. Rewrite (4.4) as $h_2'' + gh_2' - h_1h_2 = 0$ for all $\xi \geqslant 0$, since $h_2(\eta) = h_2'(\eta) = 0$, by the uniqueness theorem of solutions to the ODE, then $h_2(\xi) = 0$ for all $\xi \geqslant 0$, which implies that $B = h_3(0) = h_2'(0) = 0$, this leads to a contradiction. Since $h_4(\xi) \geqslant 0$ for all $\xi \geqslant \eta$, then there exists some $\beta \in (\eta, \alpha)$ such that $h_4(\beta) > 0$. Since $\left(e^{\int_\eta^\xi g(t)\mathrm{d}t} h_4(\xi)\right)' \geqslant 0$ for all $\xi \geqslant 0$ and $h_4(\beta) > 0$, then $h_4(\xi) > 0$ for all $\xi > \beta$. Since $\alpha > \beta$, then $h_4(\beta) < h_4(\alpha) = 0$, this leads to a contradiction. Therefore, we know that $h_4(\xi) > 0$ for all $\xi > \eta$. □

Since $h_4(\xi_0) = h_4(\eta) = 0$, $\xi_0 \geqslant \eta$, by Claim 4.4, then $\xi_0 = \eta$. By the definition of η and Claim 4.4, then $h_4(\xi) < 0$ for all $0 \leqslant \xi < \xi_0$ and $h_4(\xi) > 0$ for all $\xi > \xi_0$. □

Proposition 4.5 Assume that $A > 0$ and $B > 0$, if $g^{(4)}(\xi) < 0$ for all $\xi \geqslant 0$, then $g'''(\xi) > 0$ for all $\xi \geqslant 0$. In particular, since $g''(0) = A > 0$, then $g''(\xi) > A > 0$ for all $\xi > 0$. Moreover, since $g'(0) = 0$, then $g'(\xi) > 0$ for all $\xi > 0$.

Proof. If not, since $h_3(0) = B > 0$ and $h_4(\xi) < 0$ for all $\xi \geqslant 0$, then there exists a unique $x_0 > 0$ such that $h_3(\xi) > 0$ for all $0 \leqslant \xi < x_0$, $h_3(x_0) = 0$ and $h_3(\xi) < 0$ for all $\xi > x_0$. Since $h_2(0) = A > 0$ and $h_3(\xi) > 0$ for all $0 \leqslant \xi < x_0$, then $h_2(\xi) > 0$ for all $0 \leqslant \xi \leqslant x_0$. Since $h_1(0) = 0$, then $h_1(\xi) > 0$ for all $0 \leqslant \xi \leqslant x_0$, which implies that $h_1(x_0)h_2(x_0) > 0$. Since $h_3(x_0) = 0$ and $h_4(\xi) < 0$ for all $\xi \geqslant 0$, by (4.4), we know that $h_1(x_0)h_2(x_0) = h_4(x_0) - g(x_0)h_3(x_0) = h_4(x_0) < 0$, this leads to a contradiction. □

Proposition 4.6 Assume that $A > 0$ and $B > 0$, and there exists some $\xi_0 > 0$ such that $g^{(4)}(\xi) < 0$ for all $\xi \in (0, \xi_0)$ and $g^{(4)}(\xi) > 0$ for all $\xi > \xi_0$. Then ξ_0 is the unique global minimum point of $g'''(\xi)$ on $[0, \infty)$ and $g'''(\xi_0) > 0$. In particular, since $g''(0) = A > 0$, then $g''(\xi) > A > 0$ for all $\xi > 0$. Moreover, since $g'(0) = 0$, then $g'(\xi) > 0$ for all $\xi > 0$.

Proof. Since $g^{(4)}(\xi) < 0$ for all $\xi \in (0, \xi_0)$ and $g^{(4)}(\xi) > 0$ for all $\xi > \xi_0$, then $g'''(\xi)$ is strictly decreasing on $[0, \xi_0]$ and strictly increasing on $[\xi_0, +\infty)$, which implies that ξ_0 is the unique global minimum point of $g'''(\xi)$ on $[0, \infty)$. Now let us decide the sign of $h_3(\xi_0) = g'''(\xi_0)$. If $h_3(\xi_0) \leqslant 0$, since $h_3(0) = B > 0$ and $g^{(4)}(\xi) < 0$ for all $\xi \in [0, \xi_0)$, then there exists a unique $\eta \in (0, \xi_0]$ such that $h_3(\xi) > 0$ for all $0 \leqslant \xi < \eta$, $h_3(\eta) = 0$ and $h_3(\xi) < 0$ for all $\xi_0 > \xi > \eta$. Since $h_2(0) = A > 0$, then $h_2(\xi) > A > 0$ for all $0 \leqslant \xi \leqslant \eta$. Since $h_1(0) = 0$, then $h_1(\xi) > 0$ for all $0 \leqslant \xi \leqslant \eta$, which implies that $h_1(\eta)h_2(\eta) > 0$. Since $h_3(\eta) = 0$, $h_4(\xi) < 0$ for all $0 \leqslant \xi < \xi_0$ and $0 \leqslant \eta \leqslant \xi_0$, by (4.4), we know that $h_1(\eta)h_2(\eta) = h_4(\eta) - g(\eta)h_3(\eta) = h_4(\eta) \leqslant 0$, this leads to a contradiction. □

Proposition 4.7 Assume that $A < 0$ and $B > 0$, and $g^{(4)}(\xi) < 0$ for all $\xi \geqslant 0$.

(a) If $g'''(x_0) = 0$ for some $x_0 > 0$, then there is no point $\zeta > 0$ such that $g'(\zeta) = 0$ and $g(\zeta) > 0$. In particular, there is no point $\zeta > x_0$ such that $g'(\zeta) = 0$ and $g(\zeta) > 0$.

(b) If $g'''(\xi) > 0$ for all $\xi \geqslant 0$, then there is no point $\zeta > 0$ such that $g'(\zeta) = 0$ and $g(\zeta) > 0$.

Proof. (a) If there exists some $\zeta > 0$ such that $g'(\zeta) = 0$ and $g(\zeta) > 0$, since $h_4(\xi) < 0$ for all $\xi \geqslant 0$, by (4.4), then $h_4(\zeta) = h_1(\zeta)h_2(\zeta) - g(\zeta)h_3(\zeta) = -g(\zeta)h_3(\zeta) < 0$. Since $g(\zeta) > 0$, then $h_3(\zeta) > 0$. Since $h_4(\xi) < 0$ for all $\xi \geqslant 0$ and $h_3(x_0) = 0$, then $0 < \zeta < x_0$. Since $g'(0) = g'(\zeta) = 0$, by Lagrange's mean value theorem, then $h_2(\eta) = 0$ for some $\eta \in (0, \zeta)$. Since $h_4(\xi) < 0$ for all $\xi \geqslant 0$ and $h_3(x_0) = 0$, then $h_3(\xi) > 0$ for all $\xi \in [0, x_0)$ and $h_3(\xi) < 0$ for all $\xi > x_0$, which implies that $h_2(\xi)$ is strictly increasing on $[0, x_0]$ and strictly decreasing on $[x_0, +\infty)$. Hence x_0 is the unique global maximum point of $h_2(\xi)$ on $[0, +\infty)$. Since $h_2(\eta) = 0$, then $h_2(x_0) > 0$. Since $h_4(\xi) < 0$ for all $\xi \geqslant 0$ and $h_3(x_0) = 0$, by (4.4), then $h_4(x_0) = h_1(x_0)h_2(x_0) - g(x_0)h_3(x_0) = h_1(x_0)h_2(x_0) < 0$. Since $h_2(x_0) > 0$, then $h_1(x_0) < 0$. Since $h_3(\xi) > 0$ for all $\xi \in [0, x_0)$, then $h_2(\xi) < 0$ for all $\xi \in [0, \eta)$ and $h_2(\xi) > 0$ for all $\xi \in (\eta, x_0)$, which implies that $h_1(\xi)$ is strictly decreasing on $[0, \eta)$ and strictly increasing on (η, x_0). Since $h_1(0) = 0$, then $h_1(\xi) < 0$ for all $\xi \in (0, x_0)$. Since $\zeta \in (0, x_0)$, then $g'(\zeta) = h_1(\zeta) < 0$, this leads to a contradiction.

(b) If there exists some $\zeta > 0$ such that $g'(\zeta) = 0$ and $g(\zeta) > 0$, since $g'(0) = 0$, by Lagrange's mean value theorem, then $h_2(\eta) = 0$ for some $\eta \in (0, \zeta)$. Since $h_3(\xi) > 0$ for all $\xi \geqslant 0$, then $h_2(\xi) < 0$ for all $\xi \in [0, \eta)$ and $h_2(\xi) > 0$ for all $\xi > \eta$, which implies that $h_1(\xi)$ is strictly decreasing on $[0, \eta]$ and strictly increasing on $[\eta, +\infty)$. Since $\eta < \zeta$ and $h_1(0) = h_1(\zeta) = 0$, then $h_1(\xi) < 0$ for all $0 < \xi < \zeta$ and $h_1(\xi) > 0$ for all $\xi > \zeta$, which implies that ζ is the unique global minimum point of $g(\xi)$ on $[0, +\infty)$. Since $\Delta := g(\zeta) > 0$, then $g(\xi) \geqslant \Delta > 0$ for all $\xi \geqslant 0$. Since $h_4(\xi) < 0$ for all $\xi \geqslant 0$, by (4.5), then $h_5(\xi) = (h_2(\xi))^2 - g(\xi)h_4(\xi) > 0$ for all $\xi \geqslant 0$. Since $h_3(\xi) > 0$ and $h_4(\xi) < 0$ for all $\xi \geqslant 0$, then there exists some $L \geqslant 0$ such that $\lim_{\xi \to +\infty} h_3(\xi) = L$ and $h_3(\xi) > L \geqslant 0$ for all $\xi \geqslant 0$. By Lagrange's mean value theorem, there exists some sequence $\{y_n\}_{n=1}^{\infty}$ such that $\lim_{n\to\infty} y_n = +\infty$ and $\lim_{n\to\infty} h_4(y_n) = 0$. Since $h_5(\xi) > 0$ for all $\xi \geqslant 0$, then $h_4(\xi)$ is strictly increasing on $[0, +\infty)$, which implies that $\lim_{\xi\to+\infty} h_4(\xi) = 0$. By Lagrange's mean value theorem, there exists some sequence $\{x_n\}_{n=1}^{\infty}$ such that $\lim_{n\to\infty} x_n = +\infty$ and $\lim_{n\to\infty} h_5(x_n) = 0$. Since $g(\xi) > 0$ and $h_4(\xi) < 0$ for all $\xi \geqslant 0$, then $\limsup_{n\to\infty}[h_5(x_n) + g(x_n)h_4(x_n)] \leqslant 0$. On the other hand, since $h_2(\xi) > 0$ for all $\xi > \eta$ and $h_3(\xi) > 0$ for all $\xi \geqslant 0$, then $\limsup_{n\to\infty} (h_2(x_n))^2 > 0$, which contradicts with (4.5). □

PROPOSITION 4.8 Assume that $A < 0$ and $B > 0$, and there exists some $\xi_0 > 0$ such that $g^{(4)}(\xi) < 0$ for all $\xi \in (0, \xi_0)$ and $g^{(4)}(\xi) > 0$ for all $\xi > \xi_0$.

(a) If $g'''(x_0) \geqslant 0$ for some $x_0 \geqslant \xi_0$, then there is no point $\zeta > x_0$ such that $g'(\zeta) = 0$ and $g(\zeta) > 0$. In particular, if $g'''(\xi_0) \geqslant 0$, then there is no point $\zeta > \xi_0$ such that $g'(\zeta) = 0$ and $g(\zeta) > 0$.

(b) If $g'''(\xi) < 0$ for all $\xi \in [\xi_0, \infty)$ and $g''(\xi)$ has only one zero on $[0, \infty)$, then there is no point $\zeta > \xi_0$ such that $g'(\zeta) = 0$ and $g(\zeta) > 0$.

(c) If $g'''(\xi) < 0$ for all $\xi \in [\xi_0, \infty)$ and $g''(\alpha) = 0$ and $g'(\alpha) > 0$ for some point $\alpha > \xi_0$, then there exists a unique $\zeta > \alpha$ such that $g'(\zeta) = 0$ and $g(\zeta) > 0$. In particular, there exists a unique $\gamma \in (0, \zeta)$ such that $g'(\gamma) = 0$. If $\gamma < \xi_0$, then $g(\gamma) < 0$. If $\gamma > \xi_0$, then $g(\gamma) > 0$.

Proof. (a) Assume that there is some point $\zeta > x_0$ such that $g'(\zeta) = 0$ and $g(\zeta) > 0$, since $h_4(\xi) = g^{(4)}(\xi) > 0$ for all $\xi > \xi_0$ and $g'''(x_0) \geqslant 0$, then $h_3(\zeta) > 0$. Since $h_4(\xi) > 0$ for all $\xi > \xi_0$, by (4.4), then $h_4(\zeta) = h_1(\zeta)h_2(\zeta) - g(\zeta)h_3(\zeta) = -g(\zeta)h_3(\zeta) > 0$. Since $g(\zeta) > 0$, then $h_3(\zeta) < 0$, this leads to a contradiction.

(b) Assume that there is some point $\zeta > \xi_0$ such that $g'(\zeta) = 0$ and $g(\zeta) > 0$, since $g'(0) = 0$, by Lagrange's mean value theorem, then there exists some $\alpha \in (0, \zeta)$ such that $h_2(\alpha) = g''(\alpha) = 0$. Since $g''(0) = A < 0$ and $g''(\xi)$ has only one zero on $[0, \infty)$, then $h_2(\xi) < 0$ for all $\xi \neq \alpha$, which implies that α is the unique global maximum point of $g''(\xi)$. Hence $h_3(\alpha) = 0$ and $h_4(\alpha) \leqslant 0$. Since

$g^{(4)}(\xi) < 0$ for all $\xi \in (0, \xi_0)$ and $g^{(4)}(\xi) > 0$ for all $\xi > \xi_0$, then $0 < \alpha \leqslant \xi_0$. Since $h_3(\alpha) = 0$ and $h_3(\xi) = g'''(\xi) < 0$ for all $\xi \geqslant \xi_0$, then $0 < \alpha < \xi_0$, which implies that $h_4(\alpha) < 0$. On the other hand, since $h_2(\alpha) = h_3(\alpha) = 0$, by (4.4), then $h_4(\alpha) = h_1(\alpha)h_2(\alpha) - g(\alpha)h_3(\alpha) = 0$, this leads to a contradiction.

(c) Since $g^{(4)}(\xi) < 0$ for all $\xi \in (0, \xi_0)$ and $g^{(4)}(\xi) > 0$ for all $\xi > \xi_0$, then $h_3(\xi)$ is strictly decreasing on $[0, \xi_0]$ and strictly increasing on $[\xi_0, +\infty)$, which implies that ξ_0 is the unique global minimum point of $h_3(\xi)$ on $[0, +\infty)$. Since $h_3(\xi_0) < 0$, $h_3(0) = B > 0$ and $h_4(\xi) < 0$ for all $0 \leqslant \xi < \xi_0$, then there exists a unique $x_1 \in (0, \xi_0)$ such that $h_3(\xi) > 0$ for all $0 \leqslant \xi < x_1$ and $h_3(\xi) < 0$ for all $x_1 < \xi < \xi_0$. Since $h_3(\xi) < 0$ for all $\xi \geqslant \xi_0$, then $h_3(\xi) > 0$ for all $0 \leqslant \xi < x_1$ and $h_3(\xi) < 0$ for all $\xi > x_1$, which implies that $h_2(\xi)$ is strictly increasing on $[0, x_1]$ and strictly decreasing on $[x_1, +\infty)$. Since $h_2(0) = A < 0$ and $h_2(\alpha) = 0$, then $h_2(\xi)$ has either 1 or 2 zeros on $[0, +\infty)$. If $h_2(\xi)$ has only one zero on $[0, +\infty)$, since $h_2(0) = A < 0$ and $h_2(\alpha) = 0$, then α is the only global maximum point of $h_2(\xi)$ on $[0, +\infty)$. Since $h_2(\xi)$ is strictly increasing on $[0, x_1]$ and strictly decreasing on $[x_1, +\infty)$, then $\alpha = x_1$, which implies that $\alpha = x_1 < \xi_0$, this contradicts $\alpha > \xi_0$. If $h_2(\xi)$ has two zeros on $[0, +\infty)$, then there exists a unique $\beta \in (0, x_1)$ such that $h_2(\xi) > 0$ for all $\beta < \xi < \alpha$ and $h_2(\xi) < 0$ for all $\xi \in (0, \beta) \cup (\alpha, +\infty)$. Since $h_2(\xi) < 0$ for all $\xi > \alpha$ and $h_3(\xi) < 0$ for all $\xi > x_1$, then $\lim_{\xi \to +\infty} h_1(\xi) = -\infty$. Since $h_1(\alpha) = g'(\alpha) > 0$ and $h_2(\xi) < 0$ for all $\xi > \alpha$, then there exists a unique $\zeta > \alpha$ such that $h_1(\zeta) = g'(\zeta) = 0$. Since $\zeta > \alpha > \xi_0$ and $h_4(\xi) > 0$ for all $\xi > \xi_0$, by (4.4), then $h_4(\zeta) = h_1(\zeta)h_2(\zeta) - g(\zeta)h_3(\zeta) = -g(\zeta)h_3(\zeta) > 0$. Since $\zeta > \alpha > \xi_0$ and $h_3(\xi) < 0$ for all $\xi \geqslant \xi_0$, then $g(\zeta) > 0$.

Since $h_1(0) = 0$ and $h_2(\xi) < 0$ for all $0 < \xi < \beta$, then $h_1(\xi) < 0$ for all $0 < \xi \leqslant \beta$. Since $h_1(\alpha) > 0$ and $h_2(\xi)$ is strictly increasing for all $\beta < \xi < \alpha$, then there must exist a point $\gamma \in (\beta, \alpha)$ such that $h_1(\gamma) = 0$ and $h_2(\gamma) > 0$. Since $0 < x_1 < \xi_0$ and $h_4(x_1) < 0$, by (4.4), then $h_4(x_1) = h_1(x_1)h_2(x_1) - g(x_1)h_3(x_1) = h_1(x_1)h_2(x_1) < 0$. Since $h_2(x_1) > 0$, then $h_1(x_1) < 0$. Hence, it is obvious that $x_1 < \gamma < \alpha$ and $h_3(\gamma) < 0$. Since $h_1(\xi) < 0$ for all $0 < \xi < \gamma$ and $h_1(\xi) > 0$ for all $\gamma < \xi < \zeta$, then point γ is the minimum value of $g(\xi)$ on $[0, \zeta]$. Now let us decide the sign of $g(\gamma)$. Since $x_1 < \xi_0 < \alpha$, two cases will arise:

1) If $x_1 < \gamma < \xi_0$, by (4.4), then $h_4(\gamma) = h_1(\gamma)h_2(\gamma) - g(\gamma)h_3(\gamma) = -g(\gamma)h_3(\gamma) < 0$, then $g(\gamma) < 0$. Therefore, in this case, there exists a solution of (2.16) and (2.17). We will designate this solution as type *II* solution corresponding to the numerical type *II* solution in Section 3.

2) If $\xi_0 < \gamma < \alpha$, by (4.4), then $h_4(\gamma) = h_1(\gamma)h_2(\gamma) - g(\gamma)h_3(\gamma) = -g(\gamma)h_3(\gamma) > 0$, then $g(\gamma) > 0$. Therefore, in this case, there exists a solution of (2.16) and (2.17). We will designate this solution as type *III* solution corresponding to the numerical type *III* solution in Section 3. □

5. Asymptotic multiple solutions for high Reynolds number *Re*

We have shown the existence of multiple solutions and from the numerical solutions, we know that when *Re* is relatively large, there exists three solutions. Since the upper wall is with injection while the lower wall is with suction that indicates that the flow may exhibit a boundary layer structure near the lower wall for high Reynolds number, it is of considerable theoretical interest to construct asymptotic solution for the three types solutions that can help us to develop a better understanding of the characteristics of boundary layer.

By treating $\varepsilon = \frac{1}{Re}$ as a small perturbation parameter, (2.16) can be written as

$$\varepsilon f''' + (ff'' - f'^2) = k, \tag{5.1}$$

where $k = K/Re$.

5.1 *Asymptotic solution of type I*

From the numerical solution of type *I* in Fig. 3, we can see that the streamwise velocity rapidly decays near the lower wall ($y = -1$). Hence, by the method of boundary layer correction, $f(y)$ and k can be expanded as follows:

$$f(y) = f_0(y) + \varepsilon(f_1(y) + h_1(\eta)) + \varepsilon^2(f_2(y) + h_2(\eta)) + \cdots, \tag{5.2}$$

$$k = k_0 + \varepsilon k_1 + \varepsilon^2 k_2 + \cdots, \tag{5.3}$$

where $\eta = \frac{1+y}{\varepsilon}$ is a stretching transformation near $y = -1$ and $h_i(\eta)$, $i = 1, 2\cdots$ are boundary layer functions. By substituting (5.2) into (2.17) and collecting the equal powers of ε, the boundary conditions become

$$f_0|_{y=1} = 1, \quad f_0'|_{y=1} = 0, \quad f_0|_{y=-1} = a, \tag{5.4}$$

$$f_{i-1}'|_{y=-1} + \dot{h}_i|_{\eta=0} = 0, \quad i = 1, 2, \cdots, \tag{5.5}$$

$$f_i|_{y=1} = 0, \quad f_i'|_{y=1} = 0, \quad f_i|_{y=-1} + h_i|_{\eta=0} = 0, \quad i = 1, 2, \cdots, \tag{5.6}$$

where $\dot{h}_i$ denotes the derivative of h_i with respect to η. We note here that $f_0(y)$ is the solution of the reduced problem

$$f_0 f_0'' - f_0'^2 = k_0 \tag{5.7}$$

satisfying boundary conditions (5.4). The construction is similar to that of section 4.1 in Guo *et al.* (2018), where additional factors such as a magnetic force and a boundary expansion rate are considered. So we omit the details here and only provide the asymptotic solution of (2.16) and (2.17) for type *I* solution

$$\begin{aligned} f(y) = &\cos z + \varepsilon\{(Q(z) + b)\sin z + \frac{\lambda}{2b}(z\sin z + \cos z) + \frac{\lambda}{2b} + \frac{b}{2}(z\tan^2 z - \tan z) \\ &+ \frac{b}{2}(\ln(1 - \sin z) - \ln\cos z)(z\sin z + \cos z) + \frac{b}{a}\sin 2b \cdot e^{-a\eta}\} + O(\varepsilon^2), \end{aligned} \tag{5.8}$$

where $\eta = \frac{1+y}{\varepsilon}$, $z = by - b$, $b = \frac{\cos^{-1} a}{2}$, $Q(z) = b\int_0^z \phi\sec\phi(1 - \sec^2\phi)\mathrm{d}\phi$ and

$$\begin{aligned} \lambda = &\frac{1}{2a(b\sin(2b) + \cos(2b))}(2(b - ab - aQ(-2b))\sin(2b) + ab\tan(2b) \\ &- 2ab^2\tan^2(2b) + ab(\cos(2b) + 2b\sin(2b))(\ln(1 + \sin(2b)) - \ln\cos(2b))). \end{aligned}$$

REMARK 5.1 The asymptotic solution (5.8) is constructed for the case $0 < a < 1$ (where the injection is stronger than the suction). For the case $a > 1$ (where the suction is stronger than the injection), the

asymptotic solution can be constructed similarly. Hence, we neglect the details of the construction, but just present the asymptotic solution as follows:

$$f(y) = \cosh z + \varepsilon((-b + \frac{1}{2}\lambda z + Q(z))\sinh z - \frac{1}{2}\lambda\cosh z + \frac{1}{2}b\tanh z + \frac{1}{2}\lambda \mathrm{sech} z + \frac{1}{2}\lambda \sinh z \tanh z + \frac{1}{2}bz\tanh^2 z + b(\cosh z - z\sinh z)\arctan(\tanh\frac{z}{2}) - \frac{b}{a}\sinh(2b)e^{-a\eta}) + O(\varepsilon^2), \tag{5.9}$$

where $\eta = \frac{1+y}{\varepsilon}$, $z = by - b$, $b = \frac{\cosh^{-1} a}{2}$, $Q(z) = b\int_0^z \phi\,\mathrm{sech}\phi\tanh^2\phi \mathrm{d}\phi$ and

$$\lambda = \frac{1}{ab\cosh(b)\sinh(b)}(2a(Q(-2b) - b)\mathrm{csch}(2b) + 2ab^2\mathrm{sech}^2(2b) + ab\mathrm{csch}(2b)\mathrm{sech}(2b) + b\coth(b)\mathrm{sech}(2b) + b\tanh(b)\mathrm{sech}(2b)) - 4ab^2\mathrm{csch}(2b)\arctan(\tanh(b)) + 2ab\coth(2b)\mathrm{csch}(2b)\arctan(\tanh(b)).$$

5.2 *Asymptotic solution of type II*

Constructing an asymptotic expansion as $Re \to \infty$ for the solution of type *II* is a more complicated process than that presented in the previous subsection. From Fig. 4(a), we know that $f(y)$ vanishes at exactly two points y_1 in $(-1, 0)$ and y_2 in $(0, 1)$ (called turning points), then there may exist an interior layer near the zero of f closest to $y = -1$ and an interior layer near the zero of f closest to $y = 1$. Meanwhile, from Fig. 4(b), we see that there may exist a boundary layer near $y = -1$ since the lower wall is with suction. Cox & King (2004) give a more systematic asymptotic treatment, for the problem with interior layer and boundary layer, than that of MacGillivray & Lu (1994). In our problem, there exists an interior layer near the zero of $f(y)$ closest to $y = 1$ but does not exist a boundary layer near $y = 1$. We thus adopt the MacGillivray & Lu (1994) approach to deal with the interior layer solution and the boundary conditions at $y = 1$. Hence, the technique used in this section follows the symmetric flow case in MacGillivray & Lu (1994) and Lu (1997, 1999a) where there exists only one turning point.

Define that the distance between $y = -1$ and $y = y_1$ is Δ_1 and the distance between $y = 1$ and $y = y_2$ is Δ_2, hence, it follows that $y_1 = -1 + \Delta_1$ and $y_2 = 1 - \Delta_2$ which are unknown a priori. By differentiating (5.1), we obtain

$$\varepsilon f^{iv} + (ff''' - f'f'') = 0. \tag{5.10}$$

1) Asymptotic solution between the turning points y_1 and y_2

Letting $\varepsilon = 0$, (5.10) becomes

$$ff''' - f'f'' = 0. \tag{5.11}$$

We observe three types of solutions for the equation: cy, $c\sinh(dy+e)$ and $c\sin(dy+e)$. But, to have the solution be valid uniformly in $[y_1, y_2]$ and satisfy the conditions $f(y_1) = 0$ and $f(y_2) = 0$, the following

has to hold:

$$f(y) \sim \Lambda \sin \frac{\pi}{2-\Delta_1-\Delta_2}(y-(-1+\Delta_1)) \tag{5.12a}$$

$$= -\Lambda \sin \frac{\pi}{2-\Delta_1-\Delta_2}(y-(1-\Delta_2)), \tag{5.12b}$$

where $\Lambda < 0$ is a constant. Figure 4 shows that the turning points y_1 and y_2 are moving towards the left-end point and the right-end point of the interval $[-1, 1]$, respectively, with the increase of *Re*. The quantities Δ_1, Δ_2 and Λ which are related to ε, will be determined next by matching as $\varepsilon \to 0$.

2) Asymptotic solution near $y = y_1$ and inner solution near $y = -1$

We introduce a variable transformation

$$\tau = \frac{-1+\Delta_1-y}{\Delta_1}, \quad y \in [-1, -1+\Delta_1]. \tag{5.13}$$

Letting $f(y) = f(-1+\Delta_1-\tau\Delta_1) = \bar{f}(\tau)$, then, (5.10) becomes

$$\bar{\varepsilon}\bar{f}^{iv} - (\bar{f}\bar{f}''' - \bar{f}'\bar{f}'') = 0, \tag{5.14}$$

where $\bar{\varepsilon} = \frac{\varepsilon}{\Delta_1}$. The boundary conditions to be satisfied by (5.14) are

$$\bar{f}(0) = 0, \quad \bar{f}(1) = a, \quad \bar{f}'(1) = 0. \tag{5.15}$$

Since $\bar{\varepsilon} \to 0$ as $\varepsilon \to 0$, (5.14) subject to (5.15) is still a singular perturbation problem.

(**1**) Outer solution

Setting $\bar{\varepsilon} = 0$, the reduced equation is

$$\bar{f}\bar{f}''' - \bar{f}'\bar{f}'' = 0, \tag{5.16}$$

satisfying the boundary condition $\bar{f}(0) = 0, \bar{f}(1) = a$ and $\bar{f}'(\tau) > 0$ for all τ. Equation (5.16) may have three possible solutions: $\sigma\tau$, $a \sin \frac{\pi}{2}\tau$ and $a \sinh(\ln(\frac{1+\sqrt{5}}{2})\tau)$. By the proof of Proposition 4.8(c) for the type *II* solution, we know that $\frac{1}{2}b(y_1+1) < \gamma < \xi_0$, then $g^{iv}(\xi) < 0$ in $(0, \frac{1}{2}b(y_1+1))$, thus $\bar{f}^{iv}(\tau) < 0$ in $(0, 1)$. Hence, trigonometric functions and hyperbolic functions can be excluded. The outer solution is

$$\bar{f}(\tau) = \sigma\tau + \cdots, \tag{5.17}$$

where σ will be determined by matching.

(**2**) Inner solution

The lower wall of the channel is with suction, hence, we introduce a stretching variable $x^* = \frac{1-\tau}{\bar{\varepsilon}}$. Letting $\bar{f}(\tau) = \widehat{f}(x^*)$, then, (5.14) becomes

$$\widehat{f}'''' + \widehat{f}\widehat{f}''' - \widehat{f}'\widehat{f}'' = 0. \tag{5.18}$$

The conditions at point $x^* = 0$ are $\widehat{f}(0) = a$ and $\widehat{f}'(0) = 0$. The inner solution can be expanded as:

$$\widehat{f}(x^*) = a + \overline{\varepsilon}\widehat{f}_1(x^*) + \cdots. \tag{5.19}$$

Substituting (5.19) into (5.18) and collecting the terms of $O(\overline{\varepsilon})$, we can obtain the equation of $\widehat{f}_1(x^*)$

$$\widehat{f}_1^{iv} + a\widehat{f}_1''' = 0, \tag{5.20}$$

satisfying $\widehat{f}_1(0) = \widehat{f}_1'(0) = 0$. Then, the expression of $\widehat{f}_1(x^*)$ is

$$\widehat{f}_1(x^*) = b_1(e^{-ax^*} + ax^* - 1) + b_2 x^{*2}, \tag{5.21}$$

where b_1 and b_2 will be determined by matching. Hence, the inner solution becomes

$$\widehat{f}(x^*) = a + \overline{\varepsilon}(b_1(e^{-ax^*} + ax^* - 1) + b_2 x^{*2}) + \cdots. \tag{5.22}$$

Meanwhile, assume that the expression of outer solution can be written as

$$\overline{f}(\tau) = \sigma\tau + \overline{\varepsilon}\overline{f}_1(\tau) + \overline{\varepsilon}^2\overline{f}_2(\tau) + \cdots. \tag{5.23}$$

Substituting (5.23) into (5.14) yields that $\overline{f}_1(\tau)$ satisfies

$$\tau\overline{f}_1''' - \overline{f}_1'' = 0. \tag{5.24}$$

The corresponding condition is $\overline{f}_1(0) = 0$. Then, the expression of $\overline{f}_1(\tau)$ is

$$\overline{f}_1(\tau) = \frac{1}{6}c_1\tau^3 + d_1\tau, \tag{5.25}$$

where c_1 and d_1 are constants. The outer solution (5.23) expressing in terms of inner variable x^* is

$$\begin{aligned}\overline{f}(\tau) &= \sigma(1 - \overline{\varepsilon}x^*) + \overline{\varepsilon}(c_1(1 - \overline{\varepsilon}x^*)^3 + d_1(1 - \overline{\varepsilon}x^*)) + \cdots \\ &= \sigma + \overline{\varepsilon}(-\sigma x^* + c_1 + d_1) + \cdots.\end{aligned} \tag{5.26}$$

Matching the inner solution (5.22) with the outer solution (5.26) gives $\sigma = a$, $b_1 = -1$, $b_2 = 0$ and $c_1 + d_1 = 0$. Following the analysis in Lu (1999a), we know that $\overline{f}_i(\tau)$ are all linear, $i = 1, 2, \cdots$, where $c_1 = 0$ and $d_1 = 1$. Hence, $\overline{f}(\tau)$ can be written as

$$\overline{f}(\tau) \sim \theta(\overline{\varepsilon})\tau, \tag{5.27}$$

where $\theta(\overline{\varepsilon}) = a + d_1\overline{\varepsilon} + d_2\overline{\varepsilon}^2 + \cdots$ and $\theta(\overline{\varepsilon}) \to a$ as $\overline{\varepsilon} \to 0$. The inner solution has exponentially small terms and outer solution has to be more precise, we assume that $\overline{f}(\tau)$ is as follow:

$$\overline{f}(\tau) = \theta(\overline{\varepsilon})\tau + \sum_{i=1}^{\infty} \delta_i h_i(\tau), \tag{5.28}$$

where $\delta_i = \delta_i(\overline{\varepsilon}) = o(\overline{\varepsilon}^n)$ and $\delta_{i+1} \ll \delta_i$ for all positive integers n and i. Equation (5.28) is valid in the small neighborhood of the turning point $y_1 = -1 + \Delta_1$. Substituting (5.28) into (5.14) and collecting the terms of $O(\delta_1)$ yield

$$\overline{\varepsilon} h_1^{iv} - \theta\tau h_1''' + \theta h_1'' = 0, \tag{5.29}$$

satisfying the condition $h_1(0) = 0$. One solution of h_1 is $h_1(\tau) = -\frac{1}{6}\tau^3 + r_1\tau$, where r_1 is a constant. Setting $\delta_2 = \delta_1^2$ and collecting the terms of $O(\delta_2)$ yield

$$\overline{\varepsilon} h_2^{iv} - \theta\tau h_2''' + \theta h_2'' + \frac{\tau^3}{3} = 0. \tag{5.30}$$

Differentiate (5.30) and multiply by the integrating factor $e^{-\frac{\theta}{2\overline{\varepsilon}}\tau^2}$, then, we can obtain

$$h_2^{iv} = -\frac{1}{\overline{\varepsilon}} e^{\frac{\theta}{2\overline{\varepsilon}}\tau^2} \int_0^{\tau} s^2 e^{-\frac{\theta}{2\overline{\varepsilon}}s^2} \mathrm{d}s - Ce^{\frac{\theta}{2\overline{\varepsilon}}\tau^2}, \tag{5.31}$$

where C is a constant. If we choose $\tau < 0$ which is away from zero, h_2^{iv} will have exponentially large term. Then, we can choose C to eliminate the exponentially large term. Evaluating (5.31) leads to

$$h_2^{iv} = -\frac{1}{\overline{\varepsilon}} e^{\frac{\theta}{2\overline{\varepsilon}}\tau^2} \{-(\frac{2\overline{\varepsilon}}{\theta})^{3/2}[\frac{\sqrt{\pi}}{4} - \frac{1}{2}\sqrt{\frac{\theta}{2\overline{\varepsilon}}}|\tau|e^{-\frac{\theta}{2\overline{\varepsilon}}\tau^2} + \cdots]\} - Ce^{\frac{\theta}{2\overline{\varepsilon}}\tau^2}. \tag{5.32}$$

Hence, we choose $C = \frac{\sqrt{2\overline{\varepsilon}\pi}}{2\theta\sqrt{\theta}}$. Evaluating (5.32), we obtain asymptotic expression

$$h_2^{iv} \sim \theta^{-1}\tau. \tag{5.33}$$

Hence, the expression for $\tau < 0$ is

$$\overline{f}(\tau) = \theta\tau + \delta_1(-\frac{\tau^3}{6} + r_1\tau) + \delta_1^2\theta^{-1}(\frac{\tau^5}{5!} + \cdots) + \cdots. \tag{5.34}$$

Then, expanding (5.12a) at the turning point $y_1 = -1 + \Delta_1$ yields

$$\begin{aligned} f(y) &\sim \Lambda \sin \frac{\pi}{2 - \Delta_1 - \Delta_2}(y - (-1 + \Delta_1)) \\ &= -\Lambda \frac{\pi\Delta_1\tau}{2 - \Delta_1 - \Delta_2} + \frac{\Lambda}{3!}(\frac{\pi\Delta_1\tau}{2 - \Delta_1 - \Delta_2})^3 - \frac{\Lambda}{5!}(\frac{\pi\Delta_1\tau}{2 - \Delta_1 - \Delta_2})^5 + \cdots. \end{aligned} \tag{5.35}$$

Comparing the linear term in (5.34) and (5.35), we can obtain

$$\Lambda \sim -\frac{a(2-\Delta_1-\Delta_2)}{\pi\Delta_1}, \tag{5.36}$$

where $\theta \sim a$ is used. Then, comparing the cubic term, we get

$$\delta_1 \sim a(\frac{\pi\Delta_1}{2-\Delta_1-\Delta_2})^2. \tag{5.37}$$

Hence, the asymptotic expansion of $\bar{f}(\tau)$ is

$$\bar{f}(\tau) = \theta\tau + a(\frac{\pi\Delta_1}{2-\Delta_1-\Delta_2})^2\frac{\tau^3}{6} + a^2(\frac{\pi\Delta_1}{2-\Delta_1-\Delta_2})^4\theta^{-1}h_2 + \cdots. \tag{5.38}$$

3) The determination of Δ_1 and Δ_2

In this section, we will find the asymptotic relationship between Δ_1, Δ_2 and ε by matching near $\tau = 1$. From (5.31) with $C = \frac{\sqrt{2\bar{\varepsilon}\pi}}{2\theta\sqrt{\theta}}$, we can know

$$h_2^{iv} = -\frac{1}{\bar{\varepsilon}}e^{\frac{\theta}{2\bar{\varepsilon}}\tau^2}\int_0^\tau s^2 e^{-\frac{\theta}{2\bar{\varepsilon}}s^2}\mathrm{d}s - \frac{\sqrt{2\bar{\varepsilon}\pi}}{2\theta\sqrt{\theta}}e^{\frac{\theta}{2\bar{\varepsilon}}\tau^2} = -\frac{\sqrt{2\bar{\varepsilon}\pi}}{\theta\sqrt{\theta}}e^{\frac{\theta}{2\bar{\varepsilon}}\tau^2} + \frac{1}{\theta}\tau + \cdots. \tag{5.39}$$

Then, from (5.38) and (5.39), we can have

$$\begin{aligned}\frac{d^4\bar{f}}{d\tau^4} &= \delta_1^2 h_2^{iv}(\tau) \\ &= -a^{1/2}\pi^{9/2}\frac{\Delta_1^{7/2}}{(2-\Delta_1-\Delta_2)^4}\sqrt{2\varepsilon}e^{\frac{\theta}{2\bar{\varepsilon}}\tau^2} + a^2(\frac{\pi\Delta_1}{2-\Delta_1-\Delta_2})^4\frac{1}{\theta}\tau + \cdots.\end{aligned} \tag{5.40}$$

The outer solution (5.40) expressing in the terms of inner variable x^* is

$$\begin{aligned}\frac{1}{\bar{\varepsilon}^4}\frac{d^4\bar{f}}{dx^{*4}} =& -a^{1/2}\pi^{9/2}\frac{\Delta_1^{7/2}}{(2-\Delta_1-\Delta_2)^4}\sqrt{2\varepsilon}e^{\frac{\theta\Delta_1}{2\varepsilon}}e^{\frac{\theta\bar{\varepsilon}}{2}x^{*2}}e^{-\theta x^*} \\ &+ a^2(\frac{\pi\Delta_1}{2-\Delta_1-\Delta_2})^4\frac{1}{\theta}(1-\bar{\varepsilon}x^*) + \cdots.\end{aligned} \tag{5.41}$$

Differentiating (5.22) four times gives

$$\frac{1}{\bar{\varepsilon}^4}\frac{d^4\bar{f}}{dx^{*4}} = -\frac{a^4}{\bar{\varepsilon}^3}e^{-ax^*} + \cdots. \tag{5.42}$$

Comparing (5.41) and (5.42) suggests that the overlap domain must satisfy the conditions: $\frac{\overline{\varepsilon}\theta}{2}x^{*2} \ll 1$ and $x^{*2} \gg 1$. It is obvious that

$$-a^{1/2}\pi^{9/2}\frac{\Delta_1^{7/2}}{(2-\Delta_1-\Delta_2)^4}\sqrt{2\varepsilon}e^{\frac{\theta\Delta_1}{2\varepsilon}} \sim -\frac{a^4}{\overline{\varepsilon}^3}. \tag{5.43}$$

Finally, setting $\theta \sim a + \overline{\varepsilon}$, we obtain the asymptotic relationship:

$$\frac{\Delta_1}{\varepsilon}e^{a\frac{\Delta_1}{\varepsilon}} = \frac{a^7(2-\Delta_1-\Delta_2)^8}{2e\pi^9\varepsilon^8}. \tag{5.44}$$

The relationship (5.44) is obtained by matching the interior layer and boundary layer that requires matching of the exponentially small term in (5.41) to the exponential term in (5.42). The exponentially small term of the form $e^{-\theta x^*}$ in (5.41) from interior layer is made more concrete. Indeed, (5.44) yields

$$\Delta_1(\varepsilon) \sim -8\varepsilon\log\varepsilon \quad as \quad \varepsilon \to 0 \tag{5.45}$$

which shows $\Delta_1 \gg \varepsilon$. The relationship between Δ_1 and Δ_2 will be obtained next in 4). Then, the values of Δ_1 and Δ_2 can be determined explicitly.

4) Asymptotic solution near $y = y_2$

In order to analyze the asymptotic behaviour near $y = y_2$, we also introduce a variable transformation

$$\eta = \frac{y-1+\Delta_2}{\Delta_2}, \quad y \in [1-\Delta_2, 1]. \tag{5.46}$$

Letting $f(y) = f(1-\Delta_2+\eta\Delta_2) = \tilde{f}(\eta)$, then, (5.10) becomes

$$\tilde{\varepsilon}\tilde{f}^{iv} + (\tilde{f}\tilde{f}''' - \tilde{f}'\tilde{f}'') = 0, \tag{5.47}$$

where $\tilde{\varepsilon} = \frac{\varepsilon}{\Delta_2}$. The boundary conditions to be satisfied by (5.47) are

$$\tilde{f}(0) = 0, \quad \tilde{f}(1) = 1, \quad \tilde{f}'(1) = 0, \tag{5.48}$$

$\tilde{\varepsilon} \to 0$ as $\varepsilon \to 0$, but there is no boundary layer near $\eta = 1$ (or $y = 1$), hence, (5.14) and (5.15) form a regular perturbation problem. Setting $\tilde{\varepsilon} = 0$, the reduced equation is

$$\tilde{f}\tilde{f}''' - \tilde{f}'\tilde{f}'' = 0 \tag{5.49}$$

satisfying the boundary conditions (5.48). The corresponding solution is

$$\tilde{f}(\eta) = \sin\frac{\pi}{2}\eta. \tag{5.50}$$

Since there is no boundary layer near the upper wall of the channel, we expand $\tilde{f}(\eta)$ at the point $\eta = 0$

$$\tilde{f}(\eta) = \frac{\pi}{2}\eta - \frac{1}{3!}(\frac{\pi}{2}\eta)^3 + \frac{1}{5!}(\frac{\pi}{2}\eta)^5 + O(\tilde{\varepsilon}). \tag{5.51}$$

Then, expand (5.12b) at the turning point $y_2 = 1 - \Delta_2$

$$\begin{aligned} f(y) &\sim -\Lambda \sin \frac{\pi}{2 - \Delta_1 - \Delta_2}(y - (1 - \Delta_2)) \\ &= -\Lambda \frac{\pi \Delta_2 \eta}{2 - \Delta_1 - \Delta_2} + \frac{\Lambda}{3!}(\frac{\pi \Delta_2 \eta}{2 - \Delta_1 - \Delta_2})^3 - \frac{\Lambda}{5!}(\frac{\pi \Delta_2 \eta}{2 - \Delta_1 - \Delta_2})^5 + \cdots . \end{aligned} \tag{5.52}$$

Comparing the linear term in (5.51) and (5.52): $\frac{\pi}{2} \sim -\Lambda \frac{\pi \Delta_2}{2 - \Delta_1 - \Delta_2}$, then we can obtain

$$\Lambda \sim -\frac{2 - \Delta_1 - \Delta_2}{2\Delta_2}. \tag{5.53}$$

From (5.36) and (5.53), the relationship between Δ_1 and Δ_2 is obvious:

$$\frac{\Delta_2}{\Delta_1} = \frac{\pi}{2a}. \tag{5.54}$$

5.3 *Asymptotic solution of type III*

The numerical solution for type *III* in Fig. 5 shows that, as $Re \to \infty$, the flow should consist of an inviscid core and a thin boundary layer near the lower wall. Both transverse and streamwise velocities rapidly decay and then the streamwise velocity rapidly increases near the lower wall for type *III* solution while only streamwise velocity rapidly decays for types *I* and *II* solutions. Therefore, it is reasonable to expect that the high Reynolds number structure of the flow can be determined by boundary layer theory near the lower wall. Further, in this case we expect from numerical results that only two boundary conditions at the upper wall ($y = 1$) are satisfied by the reduced problem. This makes the construction much harder than that of type *I* solution. We expand k as (5.3) and f as follows:

$$f(y) = f_0(y) + h_0(\eta) + \varepsilon(f_1(y) + h_1(\eta)) + \varepsilon^2(f_2(y) + h_2(\eta)) + \cdots , \tag{5.55}$$

where $\eta = \frac{1+y}{\varepsilon}$ is a stretching transformation near the lower wall dimensionless height $y = -1$ and $h_i(\eta)$, $i = 0, 1, 2 \cdots$ are boundary layer functions. By substituting (5.55) into (2.17), the boundary conditions become

$$f_0|_{y=1} = 1, \quad f_0'|_{y=1} = 0, \tag{5.56}$$

$$h_0|_{\eta=0} = a - f_0|_{y=-1}, \quad \dot{h_0}|_{\eta=0} = 0, \tag{5.57}$$

$$f_i|_{y=1} = 0, \quad f_i'|_{y=1} = 0, \quad i = 1, 2, \cdots , \tag{5.58}$$

$$h_i|_{\eta=0} = -f_i|_{y=-1}, \quad \dot{h_i}|_{\eta=0} = -f_{i-1}'|_{y=-1}, \quad i = 1, 2, \cdots , \tag{5.59}$$

where $\dot{h_0}$ denotes the derivative of h_0 with respect to η. Substituting (5.55) and (5.3) into (5.1) and collecting the terms of $O(1)$, we can obtain the equation of f_0 (same as (5.7)):

$$f_0 f_0'' - f_0'^2 = k_0, \tag{5.60}$$

satisfying boundary conditions (5.56) (different from (5.4)). Similarly, collecting the terms of $O(\varepsilon^{-2})$, we can obtain the equation of h_0:

$$\dddot{h_0} + (h_0 + f_0(-1))\ddot{h_0} - \dot{h_0}^2 = 0, \tag{5.61}$$

satisfying boundary conditions (5.57).
One expression of f_0 with the boundary conditions (5.56) is

$$f_0 = \cos(by - b), \tag{5.62}$$

where b is an undetermined parameter and we denote $f_0(-1) = \cos 2b$ as β. We shall determine β such that (5.61) subject to boundary conditions (5.57) has a boundary layer solution. Usually, we request a boundary layer function to tend to zero as $\eta \to \infty$. However, for problem (5.61) with (5.57) such a solution may not exist. A rigorous proof is highly nontrivial, we will report it in a forthcoming paper. For the purpose of the construction of the first-order asymptotic solution here in the paper, it is enough to request a boundary layer function $h_0(2/\varepsilon) \to 0$ (or much smaller than $O(\varepsilon)$) when ε is sufficiently small. It is obvious that $h_0(\eta) = a - \beta$ and $(a - \beta)e^{-\beta\eta}$ are two solutions of (5.61), but the former is not a boundary layer function and the latter does not satisfy (5.57). It is hardly possible, however, to obtain any other explicit solution for the nonlinear (5.61) with (5.57). We thus make use of both analytic and numerical tools to predict β.

Next, we shall show that $\beta < 0$ is impossible.

PROPOSITION 5.1 Let $h_0(\eta)$ be a boundary layer function solution of (5.61) and (5.57) in $[0, 2/\varepsilon)$, then we can have:

(a) If $h_0''(\eta_1) > 0$ for some $\eta_1 \geqslant 0$, then $h_0''(\eta) > 0$ for all $\eta \geqslant \eta_1$.

(b) There holds that $h_0'(\eta) \leqslant 0$ for all $\eta \geqslant 0$.

(c) There holds that $h_0'(\eta) < 0$ for all $\eta > 0$.

(d) There exists some $\eta_2 > 0$ such that $h_0''(\eta) > 0$ for all $\eta \geqslant \eta_2$.

(e) $\beta < 0$ is impossible.

Proof. (a) Let $h_2(\eta) = h_0''(\eta)$ for all $\eta \geqslant 0$, by (5.61), then $h_2' + (h_0 + \beta)h_2 = (h_0')^2 \geqslant 0$ for all $\eta \geqslant 0$, which implies that $\left(e^{\int_{\eta_1}^{\eta}(h_0(t)+\beta)\mathrm{d}t}h_2(\eta)\right)' \geqslant 0$ for all $\eta \geqslant \eta_1$. So we get $e^{\int_{\eta_1}^{\eta}(h_0(t)+\beta)\mathrm{d}t}h_2(\eta) \geqslant h_2(\eta_1) = h_0''(\eta_1) > 0$ for all $\eta \geqslant \eta_1$, which implies that $h_0''(\eta) = h_2(\eta) > 0$ for all $\eta \geqslant \eta_1$.

(b) If not, that is, there exists some $\lambda_0 > 0$ such that $h_0'(\lambda_0) > 0$. Since $h_0'(0) = 0$, then there exists some $b \in [0, \lambda_0)$ such that $h_0'(b) = 0$ and $h_0'(\eta) > 0$ for all $\eta \in (b, \lambda_0]$. Then $h_0''(b) > 0$. By the result of part (a), then $h_0''(\eta) > 0$ for all $\eta \geqslant b$, which implies that $h_0'(\eta)$ is increasing in $[b, 2/\varepsilon)$. So $h_0'(\eta) \geqslant h_0'(\lambda_0) := \sigma > 0$ for all $\eta \geqslant \lambda_0$, which implies that $h_0(\eta) - h_0(\lambda_0) \geqslant \sigma(\eta - \lambda_0)$ for all $\eta \geqslant \lambda_0$.

Since $\sigma > 0$, by taking $\eta \to 2/\varepsilon$ sufficiently large (or ε sufficiently small), then $h_0(2/\varepsilon)$ is large, and then is in contradiction to a boundary layer function.

(c) If not, by the result of part (b), then there exists some $\lambda_1 > 0$ such that $0 = h_0'(\lambda_1) = \sup_{\eta \geqslant 0} h_0'(\eta)$, which implies that $h_0''(\lambda_1) = 0$. By the uniqueness theorem of solution to ODE, then $h_0 = h_0(\lambda_1)$ $[0, 2/\varepsilon)$, and then is in contradiction to a boundary layer function.

(d) If not, that is, $h_0''(\eta) \leqslant 0$ for all $\eta \geqslant 0$, then $h_0'(\eta)$ is non-increasing on $[0, 2/\varepsilon)$. By the result of part (c), then $h_0'(\eta) \leqslant h_0'(1) < 0$ for all $\eta \geqslant 1$, which implies that $h_0(\eta) - h_0(1) \leqslant h_0'(1)(\eta - 1)$ for all $\eta \geqslant 1$. Since $h_0'(1) < 0$, by taking $\eta \to 2/\varepsilon$ sufficiently large, then $h_0(2/\varepsilon)$ is negatively large, and then is in contradiction to a boundary layer function.

(e) If not, that is $\beta < 0$, since $h_0(2/\varepsilon)$ is sufficiently small as ε is sufficiently small, then when $\eta < 2/\varepsilon$ is sufficiently large (say $\eta > \eta_3 > \eta_2$), we have $\beta + h_0(\eta) < 0$ for all $\eta > \eta_3$. From (5.61), we have

$$h_0''(\eta) = h_0''(\eta_3) e^{-\int_{\eta_3}^{\eta} (h_0(t)+\beta)\mathrm{d}t} + \int_{\eta_3}^{\eta} h_0'^2(s) e^{-\int_{s}^{\eta} (h_0(t)+\beta)\mathrm{d}t} \mathrm{d}s. \tag{5.63}$$

We mark the right most term as $B(\eta)$. Integrating (5.63) from η_3 to η, we can obtain

$$h_0'(\eta) = h_0'(\eta_3) + h_0''(\eta_3) \int_{\eta_3}^{\eta} e^{-\int_{\eta_3}^{x} (h_0(t)+\beta)\mathrm{d}t} \mathrm{d}x + \int_{\eta_3}^{\eta} B(x)\mathrm{d}x. \tag{5.64}$$

Fixed η_3, it is obvious that the first term at the right hand of (5.64) is a negative constant and the third term is always positive. Since $\beta + h_0(\eta) < 0$, by the results of parts (a) and (d), $h_0''(\eta_3) > 0$, then we have $h_0''(\eta_3) \int_{\eta_3}^{\eta} e^{-\int_{\eta_3}^{x} (h_0+\beta)\mathrm{d}t} \mathrm{d}x \geqslant h_0''(\eta_3)(\eta - \eta_3)$. Hence, $h_0'(\eta)$ is sufficiently large as η is close to $2/\varepsilon$, then $h_0(2/\varepsilon)$ cannot be close to 0, in contradiction to a boundary layer function. □

Although we can prove $\beta \geqslant 0$, it is still difficult to determine β analytically. We thus determine β numerically. Gradually increasing *Re* and comparing the type *III* numerical solution of (5.1) and (2.17) for a given boundary condition value a with the solution of the reduced problem as in expression (5.62), we can numerically estimate β. The results are summarized in Table 1. Then, it is obvious that $b = \frac{\cos^{-1}\beta}{2}$. Then, we can solve the boundary layer (5.61) subject to (5.57) numerically. The numerical results for $h_0(\eta)$ show that $h_0(\eta) \to 0$ as $\eta \to 2/\varepsilon$. Finally, the asymptotic solution up to $O(\varepsilon)$ is $f(y) = f_0(y) + h_0(\eta) + O(\varepsilon)$. This will be compared with the numerical solution in next section.

6. Comparisons of numerical and asymptotic solutions

Numerical solutions for (2.16) and (2.17) can be readily obtained by MATLAB boundary value problem solver bvp4c. Comparisons of the asymptotic solutions and numerical solutions will be shown in the following tables. To develop a better understanding of the accuracy of asymptotic solutions constructed in Section 5, we also graphically show the streamwise velocity profiles $f'(y)$ or transverse velocity profiles $f(y)$ over different ranges of Reynolds numbers at some fixed asymmetric parameter.

TABLE 1 *The numerical results of β at different given boundary condition values a for Re = 1500.*

a	0.9	0.8	0.7	0.6	0.5	0.4	0.3
β	0.0889	0.0783	0.0672	0.0551	0.0417	0.0264	0.0079

TABLE 2 *Comparison between numerical and asymptotic results for $f'(y)$ at $a = 0.5$ with $Re = 50$, $Re = 75$ and $Re = 100$.*

$f'(y)$	$Re = 50$		$Re = 75$		$Re = 100$	
y	Numeric	Asymptotic	Numeric	Asymptotic	Numeric	Asymptotic
-1.0	0.0000	0.0000	0.0000	0.0000	0.0000	0.0000
-0.8	0.4348	0.4342	0.4322	0.4324	0.4302	0.4304
-0.6	0.4015	0.4024	0.3976	0.3979	0.3955	0.3957
-0.4	0.3622	0.3629	0.3584	0.3587	0.3564	0.3566
-0.2	0.3186	0.3193	0.3151	0.3154	0.3134	0.3135
-0.0	0.2714	0.2720	0.2683	0.2686	0.2667	0.2669
0.2	0.2211	0.2215	0.2185	0.2186	0.2171	0.2172
0.4	0.1681	0.1684	0.1661	0.1662	0.1650	0.1651
0.6	0.1132	0.1134	0.1118	0.1119	0.1111	0.1111
0.8	0.0570	0.0571	0.0562	0.0563	0.0559	0.0559
1.0	0.0000	0.0000	0.0000	0.0000	0.0000	0.0000

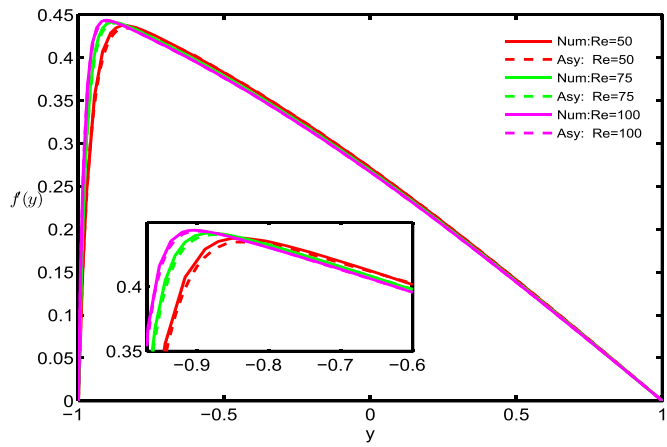

FIG. 7. Comparison between numerical and asymptotic solutions for $f'(y)$ at $a = 0.5$ with $Re = 50$, $Re = 75$ and $Re = 100$. The solid lines represent numerical solutions and the dashed lines show asymptotic solutions.

For the type *I* solution, we will make comparison between numerical and asymptotic solution for $f'(y)$ so as to see the accuracy of the type *I* asymptotic solution constructed in (5.8). From Table 2, it can be seen that the asymptotic solution is matched well with the numerical solution. Furthermore, we graphically present the comparison in Figure 7, and see that the error between the numerical and asymptotic solutions is decreasing with the increase of *Re*. Hence, the results are found to be in very well agreement which indicates that the accuracy of the asymptotic solution is reliable.

For the type *II* solution, since the turning points $y_1 = -1+\Delta_1$ and $y_2 = 1-\Delta_2$ are unknown a priori, getting the values of them is very important and difficult. We will contrast numerical and asymptotic results at the turning points. The asymptotic relationships of Δ_1 and Δ_2 are from (5.44) and (5.54). From Table 3, it can be seen that the error between the numerical and asymptotic results of the turning points is decreasing with the increase of *Re* and that Δ_1 and Δ_2 get smaller and smaller as *Re* increases. The comparison of numerical and asymptotic solutions for the transverse velocity profiles is shown in Fig. 8

TABLE 3 *Comparison between numerical and asymptotic results for the turning points* $y_1 = -1 + \Delta_1$ *and* $y_2 = 1 - \Delta_2$ *at* $a = 0.8$.

Re	$y_1 = -1 + \Delta_1$		$y_2 = 1 - \Delta_2$	
	Numeric	Asymptotic	Numeric	Asymptotic
100	-0.7449	-0.7315	0.5457	0.4728
200	-0.8263	-0.8227	0.6753	0.6519
400	-0.8914	-0.8921	0.7868	0.7959
600	-0.9203	-0.9202	0.8483	0.8434
800	-0.9363	-0.9363	0.8783	0.8750

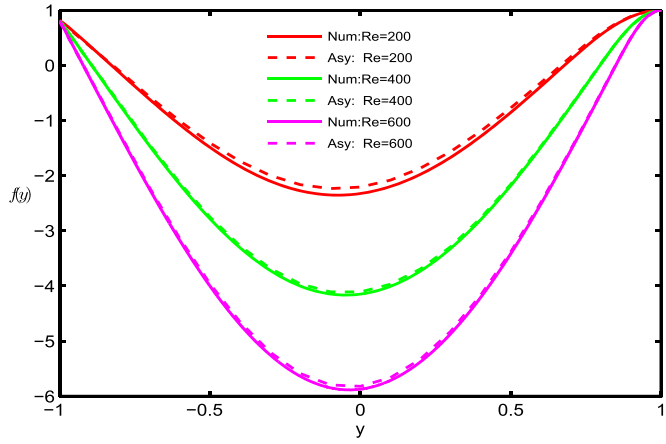

FIG. 8. Comparison between numerical and asymptotic solutions for $f(y)$ at $a = 0.8$ with $Re = 200$, $Re = 400$ and $Re = 600$. The solid lines represent numerical solutions and the dashed lines show asymptotic solutions.

(where the asymptotic solutions are from (5.38), (5.12a) or (5.12b) and (5.50)) which also indicates that the error between the numerical and asymptotic solutions is decreasing with the increase of *Re*. These verify our constructing process of the type *II* asymptotic solution in previous section.

For the type *III* solution, we will compare the numerical solution with the type *III* asymptotic solution. Because of the complexity of the boundary layer problem (5.61) and (5.57), we compute the asymptotic solution $f(y) = f_0(y) + h_0(\eta) + O(\varepsilon)$ in the following way: $f_0(y)$ is obtained from (5.62) and β or b is estimated from numerical solution of (5.1) and (2.17), and h_0 is obtained numerically based on solving (5.61) and (5.57). Table 4 shows the comparison between numerical and asymptotic solutions for transverse velocity profiles at a fixed Reynolds number *Re* with different asymmetric parameters a and Fig. 9 presents them at a fixed asymmetric parameter a with different large Reynolds numbers *Re*. They all indicate that the asymptotic solution matches well with the numerical solution for large Reynolds numbers.

7. Conclusion

In this article, we have considered the multiplicity and asymptotics of similarity solutions for laminar flows in a porous channel with different permeabilities, in particular, flows permeating from upper wall

TABLE 4 *Comparison between numerical and asymptotic solutions for $f(y)$ at $Re = 800$ with $a = 0.652$, $a = 0.748$ and $a = 0.876$.*

$f(y)$	$a = 0.652$		$a = 0.748$		$a = 0.876$	
y	Numeric	Asymptotic	Numeric	Asymptotic	Numeric	Asymptotic
-1.0	0.6520	0.6520	0.7480	0.7480	0.8760	0.8760
-0.6	0.3489	0.3462	0.3590	0.3516	0.3711	0.3586
-0.4	0.4866	0.4838	0.4948	0.4880	0.5047	0.4933
-0.2	0.6131	0.6103	0.6194	0.6133	0.6271	0.6169
0.0	0.7255	0.7228	0.7301	0.7246	0.7356	0.7267
0.2	0.8212	0.8187	0.8242	0.8196	0.8279	0.8204
0.4	0.8981	0.8959	0.8998	0.8960	0.9019	0.8960
0.6	0.9543	0.9526	0.9550	0.9523	0.9560	0.9518
0.8	0.9885	0.9875	0.9887	0.9872	0.9889	0.9867
1.0	1.0000	1.0000	1.0000	1.0000	1.0000	1.0000

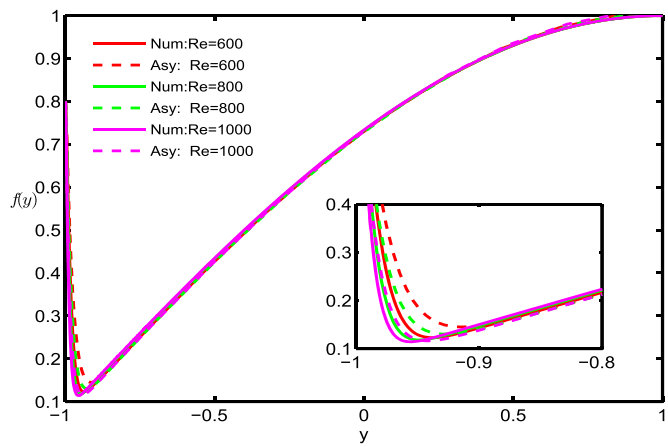

FIG. 9. Comparison between numerical and asymptotic solutions for $f(y)$ at $a = 0.8$ with $Re = 600$, $Re = 800$ and $Re = 1000$. The solid lines represent numerical solutions and the dashed lines show asymptotic solutions.

of the porous channel and exiting from the lower wall. We numerically show that there exist three solutions designated as types *I*, *II* and *III*, type *I* solution extends over $0 \leqslant Re < \infty$ and types *II* and *III* solutions appear at a common point *Re* for a fixed asymmetric parameter *a*. The value of common point *Re* is decreasing with the increase of *a*. Then, we rigorously prove that there exist three similarity solutions. Meanwhile, the asymptotic solution for each of the three types of similarity solutions is constructed for the most interesting and challenging high Reynolds number case and is also verified numerically. For the type *I* solution, its streamwise velocity has an exponentially rapid decay. For the type *II* solution, there are two turning points and its streamwise velocity also has an exponentially rapid decay. For the type *III* solution, there exists an exponentially rapid change not only for its streamwise velocity (decay and then increase) but also for its transverse velocity (decay). The reversal flow occurs for both types *II* and *III* solutions.

Acknowledgements

The authors would like to thank Professor Martin Stynes for many discussions and suggestions.

Funding

National Natural Science Foundation of China (no. 11861131004, no. 11771040, no. 11371128, no. 11801404) and by National Science Foundation-Division of Mathematical Sciences, grant number 1601885.

References

Berman, A. S. (1953) Laminar flow in channels with porous walls. *J. Appl. Phys.*, **24**, 1232–1235.

Bouyges, M., Chedevergne, F., Casalis, G. & Majdalani, J. (2017) Asymptotically based self-similarity solution of the Navier–Stokes equations for a porous tube with a non-circular cross-section. *J. Fluid Mech.*, **826**, 396–420.

Brady, J. & Acrivos, A. (1981) Steady flow in a channel or tube with an accelerating surface velocity. An exact solution to the Navier–Stokes equations with reverse flow. *J. Fluid Mech.*, **112**, 127–150.

Brady, J. F. (1984) Flow development in a porous channel and tube. *Phys. Fluids*, **27**, 1061–1067.

Chellam, S. & Liu, M. (2006) Effect of slip on existence, uniqueness, and behavior of similarity solutions for steady incompressible laminar flow in porous tubes and channels. *Phys. Fluids*, **18**, 083601–083610.

Cox, S. M. (1991a) Analysis of steady flow in a channel with one porous wall, or with accelerating walls. *SIAM J. Appl. Math.*, **51**, 429–438.

Cox, S. M. (1991b) Two-dimensional flow of a viscous fluid in a channel with porous walls. *J. Fluid Mech.*, **227**, 1–33.

Cox, S. M. & King, A. C. (1997) On the asymptotic solution of a high-order nonlinear ordinary differential equation. *Proc. R. Soc. Lond. A Math. Phys.*, **453**, 711–728.

Cox, S. M. & King, J. R. (2004) Large-Reynolds-Number asymptotics of the Berman problem. *Stud. Appl. Math.*, **113**, 217–243.

Dauenhauer, E. C. (2003) Exact self-similarity solution of the Navier–Stokes equations for a porous channel with orthogonally moving walls. *Phys. Fluids*, **15**, 1485–1495.

Dinarvand, S. & Rashidi, M. M. (2010) A reliable treatment of a homotopy analysis method for two-dimensional viscous flow in a rectangular domain bounded by two moving porous walls. *Nonlinear Anal. Real World Appl.*, **11**, 1502–1512.

Durlofsky, L. & Brady, J. F. (1998) The spatial stability of a class of similarity solutions. *Phys. Fluids*, **27**, 1068–1076.

Guo, H., Lin, P. & Lin, L. I. (2018) Asymptotic solutions for the asymmetric flow in a channel with porous retractable walls under a transverse magnetic field. *Appl. Math. Mech. (English Ed.)*, **39**, 1147–1164.

Hastings, S., Lu, C. & MacGillivray, A. (1992) A boundary value problem with multiple solutions from the theory of laminar flow. *SIAM J. Math. Anal.*, **23**, 201–208.

King, J. & Cox, S. (2001) Asymptotic analysis of the steady-state and time-dependent Berman problem. *J. Engrg. Math.*, **39**, 87–130.

King, J. R. & Cox, S. M. (2005) Self-similar 'Stagnation Point' boundary layer flows with suction or injection. *Stud. Appl. Math.*, **115**, 73–107.

Lu, C. (1997) On the asymptotic solution of laminar channel flow with large suction. *SIAM J. Math. Anal.*, **28**, 1113–1134.

Lu, C. (1999a) On matched asymptotic analysis for laminar channel flow with a turning point. *Electron. J. Differential Equations (EJDE) [electronic only]*, **03**, 109–118.

Lu, C. (1999b) On the uniqueness of laminar channel flow with injection. *Appl. Anal.*, **73**, 497–505.

Lu, C., MacGillivray, A. D. & Hastings, S. P. (1992) Asymptotic behaviour of solutions of a similarity equation for laminar flows in channels with porous walls. *IMA J. Appl. Math.*, **49**, 139–162.

MacGillivray, A. D. & Lu, C. (1994) Asymptotic solution of a laminar flow in a porous channel with large suction: a nonlinear turning point problem. *Methods Appl. Anal.*, **1**, 229–248.

Majdalani, J. & Zhou, C. (2003) Moderate-to-large injection and suction driven channel flows with expanding or contracting walls. *Z. Angew. Math. Mech.*, **83**, 181–196.

Proudman, I. (1960) An example of steady laminar flow at large Reynolds number. *J. Fluid Mech.*, **9**, 593–602.

Raithby, G. (1971) Laminar heat transfer in the thermal entrance region of circular tubes and two-dimensional rectangular ducts with wall suction and injection. *Int. J. Heat Mass Transf.*, **14**, 223–243.

Robinson, W. (1976) The existence of multiple solutions for the laminar flow in a uniformly porous channel with suction at both walls. *J. Engrg. Math.*, **10**, 23–40.

Sellars, J. R. (1955) Laminar flow in channels with porous walls at high suction Reynolds numbers. *J. Appl. Phys.*, **26**, 489–490.

Shih, K.-G. (1987) On the existence of solutions of an equation arising in the theory of laminar flow in a uniformly porous channel with injection. *SIAM J. Appl. Math.*, **47**, 526–533.

Shrestha, G. (1967) Singular perturbation problems of laminar flow through channels in a uniformly porous channel in the presence of a transverse magnetic field. *Quart. J. Mech. Appl. Math.*, **20**, 233–246.

Shrestha, G. & Terrill, R. (1968) Laminar flow with large injection through parallel and uniformly porous walls of different permeability. *Quart. J. Mech. Appl. Math.*, **21**, 413–432.

Skalak, F. M. & Wang, C. Y. (1978) On the nonunique solutions of laminar flow through a porous tube or channel. *SIAM J. Appl. Math.*, **34**, 535–544.

Terrill, R. (1965) Laminar flow in a uniformly porous channel with large injection. *Aeronaut. Quart.*, **16**, 323–332.

Terrill, R. & Shrestha, G. (1964) Laminar flow through channels with porous walls and with an applied transverse magnetic field. *Appl. Sci. Res. Sect. B*, **11**, 134–144.

Terrill, R. & Shrestha, G. (1965a) Laminar flow in a uniformly porous channel with an applied transverse magnetic field. *Appl.ied Sci. Res. Sect. B*, **12**, 203–211.

Terrill, R. & Shrestha, G. (1966) Laminar flow through a channel with uniformly porous walls of different permeability. *Appl. Sci. Res.*, **15**, 440–468.

Terrill, R. M. & Shrestha, G. M. (1965b) Laminar flow through parallel and uniformly porous walls of different permeability. *Z. Angew. Math. Phys.*, **16**, 470–482.

Uchida, S. & Aoki, H. (1977) Unsteady flows in a semi-infinite contracting or expanding pipe. *J. Fluid Mech.*, **82**, 371–387.

Varapaev, V. N. & Yagodkin, V. I. (1969) Flow stability in a channel with porous walls. *Fluid Dyn.*, **4**, 60–62.

Watson, E. B. B., Banks, W. H. H., Zaturska, M. B. & Drazin, P. G. (1990) On transition to chaos in two-dimensional channel flow symmetrically driven by accelerating walls. *J. Fluid Mech.*, **212**, 451–485.

Watson, P., Banks, W., Zaturska, M. & Drazin, P. (1991) Laminar channel flow driven by accelerating walls. *Eur. J. Appl. Math.*, **2**, 359–385.

Xu, H., Lin, Z. L., Liao, S. J., Wu, J. Z. & Majdalani, J. (2010) Homotopy based solutions of the Navier-Stokes equations for a porous channel with orthogonally moving walls. *Phys. Fluids*, **22**, 1485–136.

Yuan, S. (1956) Further investigation of laminar flow in channels with porous walls. *J. Appl. Phys.*, **27**, 267–269.

Zaturska, M., Drazin, P. & Banks, W. (1988) On the flow of a viscous fluid driven along a channel by suction at porous walls. *Fluid Dyn. Res.*, **4**, 151–178.